ISSN 2250-1967

MARINE INDIA ENGINEERS REVIEW

JOURNAL OF THE INSTITUTE OF MARINE ENGINEERS (INDIA)

Volume : 17 | Issue : 4 | March 2023 | ₹ 90/-

Page 9 **Maturity Assessment of Subsea Navigation and Positioning Systems - Part A**

Page 23 **Technological Advancement for the Use of Marine Materials in the Fields Of Super austenitics**

Page 28 **Prediction Model for the Ballast Marine Water Quality**

Assessing SUBSEA NAVIGATION Systems

The Institute of Marine Engineers (India)

IMEI HOUSE, Plot No.94, Sector-19, Nerul, Navi Mumbai.

Tel: +91 – 9967875995/ 9773363542 / 9594204403/ 022-27711663
Email: training@imare.in. Website: www.imare.in

REGISTRATION OPEN FOR Following DGS APPROVED COURSES (Online)

- Basic Training for Ships using Fuels covered within IGF code ***Course Id – 5311*** (OFFLINE) – (4 Days) - 13th March 2023 / 27th March 2023/10th April 2023/ 17th April 2023
- Assessment, Examination and Certification of Seafarers ***Course Id – 1062*** (OFFLINE) – (12 Days) - March 2023
- Advanced Training for Ships using Fuels covered within IGF code ***Course Id – 5312*** (OFFLINE) – (6 Days) - 6th March 2023/ 3rd April 2023/ 24th April 2023
- MEO Cl. I (FG) : 2- months course (OFFLINE) - 1st March 2023 / 2nd May 2023/ 1st June 2023/ 1st July 2023/ 1st August 2023/ 1st Sept.2023 (followed by Simulator course) **Discount on combined bookings of Class I Course with Simulator**
- MEO CLASS III (NCV_CEO) Upto 3000kW – STCW 2010: 2 month course (OFFLINE) 1st March 2023 / 1st July 2023/ 1st Nov. 2023
- MEO Cl. III (NCV_SEO) Part-A - STCW 2010: 2-month course (OFFLINE) – 1st August 2023
- MEO Cl. III (NCV_SEO) Part-B - STCW 2010: 4-month course (OFFLINE) – 1st April 2023 / 1st November 2023
- MEO Cl. IV (NCV) - STCW 2010 -4 months course (OFFLINE) – 1st July 2023
- MEO CL. II (FG): 4-month Course (OFFLINE) – 1st March 2023 / 1st April 2023 / 2nd May 2023 (Discount on combined bookings of Class II Courses with Simulator)
- REFRESHER & UPDATING TRAINING (RUT - 3 DAYS) COURSE FOR REVALIDATION OF COC FOR ALL ENGINEERS and ETOs (OFFLINE) –13th March 2023/ 27th March 2023/ 10th April 2023/ 24th April 2023
- ENGINE ROOM SIMULATOR MANAGEMENT LEVEL (3 DAYS) COURSE FOR MEO CLASS I (OFFLINE) – 01st March 2023/ 27th April 2023
- ENGINE ROOM SIMULATOR MANAGEMENT LEVEL (5 DAYS) COURSE FOR MEO CLASS II (OFFLINE) – 01st March 2023/ 27th March 2023/ 01st April 2023/ 24th April 2023
- ENGINE ROOM SIMULATOR OPERATIONAL LEVEL (3 DAYS) COURSE (OFFLINE) – 20th March 2023/ 17th April 2023/ 15th May 2023/ 19th June 2023
- MEO Cl. IV(FG) non mandatory course (2months duration) – On request
- 2 weeks Induction course for Naval candidates – 1st July 2023
- Familiarisation Training Course For Liquefied Natural Gas (LNG) Tanker Operations (Online) - On request

For Payment: Visit www.imare.in — Use the option "Buy Online" to pay the course fee

NOTE: Payment can be done through the ICICI Bank (IFSC Code: - ICIC0000151) on A/C No.015101031872 in the name of "The Institute of Marine Engineers (India)" only after confirming the availability of seats.

Please make the payment from saving bank account only not from NRI / NRE account

For enquiries contact on training@imare.in

For Registration of Competency Courses: https://forms.gle/DBvLuEarFpbk3aqX9

For uploading the Documents – Mail your documents on documents@imare.in after putting all documents in one pdf file

For Registration of Modular (RUT/ERS) Courses: https://forms.gle/DSmcvmMJkZAvLDvo9

Features: Experienced Faculty, Individual Attention

#WeSeaGreen with DNV

EEXI AND CII – ARE YOU READY?

Prepare now – be ready on time. DNV's technical experts and digital tools can help you take the first steps on your compliance journey. Use the EEXI Calculator to create EEXI calculations and technical files simply and quickly, gain an overview of your emissions in operation for the CII with Emissions Insights and track regulatory requirements with Compliance Planner. Let DNV help you meet the new CO_2 regulations and stay ahead of the regulatory curve.

Learn more at **dnv.com/cii**

DNV

DNV AS | Equinox Business Park, 6th Floor, Tower 3, L.B.S. Road, Kurla (W), Mumbai – 400070 | Tel: +91 22 61769000
For further seminar information please e-mail at mumbaimaritime@dnvcom

OUR VALUES

Constant Care

Humbleness

Uprightness

Our Employees

Our Name

Together All the way.

Industry Leader
Timely Relief and Assignments
Competitive Wages and Benefits
Safe Working Condition
Empowered Frontline
Attractive Workplace
Free Internet Across Entire Fleet

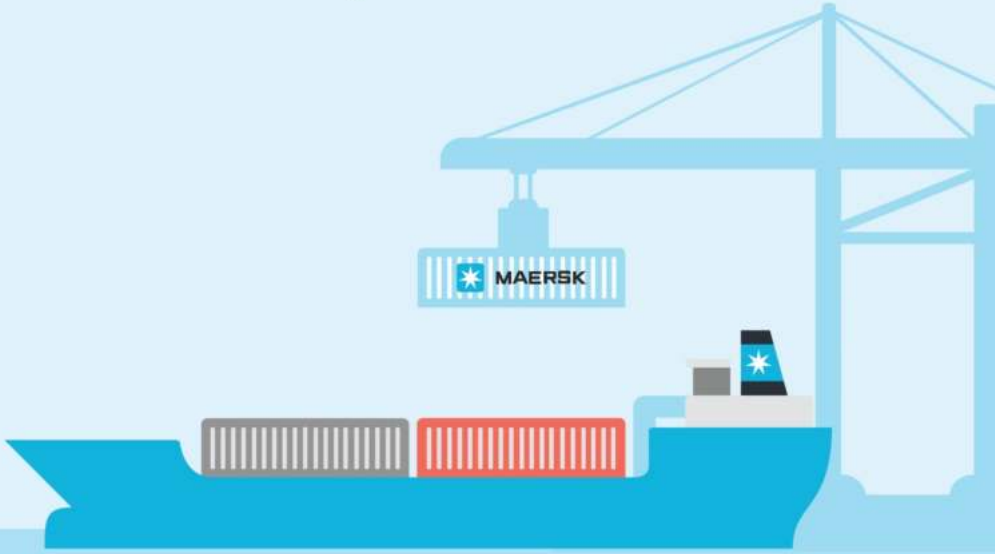

MAERSK IS RECRUITING. Apply today.

FOURTH ENGINEER
Minimum 6 months rank experience with COC

FITTER
Minimum 12 months rank experience

WIPER
Minimum 12 months rank experience

ABLE BODIED SEAMAN
Minimum 12 months rank experience on container vessel

ORDINARY SEAMAN
Minimum 12 months rank experience

SECOND COOK/GENERAL STEWARD/TRAINEE COOK
Minimum 12 months rank experience with COC

Maersk Fleet Management and Technology (I) Pvt Ltd
502 and 503, 5th Floor, Godrej 2,
PirojShah Nagar, Eastern Express Highway,
Vikhroli (East), Mumbai (MH) India 400079

Mail **MarineJobs.India@maersk.com**
Call **+91 22 50492223 / +91 124 6135752 / +91 44 66588335**
Web **maersk.com**

RPS Licence no.: RPSL-MUM-490 Valid upto 31/05/2023

MAERSK

EDITORIAL

If one does not know to which port one is sailing, no wind is favourable.
- Seneca

Industry columns were awash with expectations prior to the budget that there will be a slew of focussed measures to improve shipping, particularly to shipbuilding. The Economic Survey 2022-23, released just before the Budget, has few significant observations while emphasising the importance of nurturing shipbuilding:

- Approx. 65% of the value addition in construction (ship) is by the manufacturers of shipboard materials, equipment, and systems
- Shipbuilding has one of the highest employment multipliers (6.4)
- Shipbuilding has a robust investment multiplier at 1.82 (e.g., for an investment of 1 lakh crore, the expected circulation will be 1.82 lakh crores due to the multiplier effect)

A very important indicative parameter to note is that all these suggestive statistics are all based on shipbuilding activities pertaining to naval requirements and not connoting to building of merchant ships.

But in the Budget, infrastructure and logistics got the better of the blessings. Infrastructure-in-need for improved rail-road-waterways connectivity, freight corridors, warehousing, green logistics leverages based on green solutions, technology driven management (digitalisation)... all these will make things easier. Another move is the push toward skill and coastal enterprise development (Check: PM Yojanas [Kaushal Vikas/Matsya Sampada]). The logistics sector alone hosts over 20+ million workforce and even with all automation, India will have to still rely on the skills of the young and the not-so-young.

Looking back at the expectations, India's 30+ shipyards/13 million tonnage (approx.), could have done with some direct incentives, though the mentioned measures may be expected to generate few favourable winds for shipping also.

In all, considering the caboodle of the Budget, the port of destination appears to be the $5 trillion GDP and certainly not the Elections 2024. But if the ETA is 2025 (for the $5trillion GDP), the speeds have to be adjusted upwards. Do our economic engines pack the power for that? Times will testify.

In this issue...

We go underwater again as we start an interesting discussion on subsea navigation systems. In Part A of the series, Dr. Jyoti et al., touch on the points of development of navigation systems. The emphasis is on the subsea, underwater, autonomous vehicles' navigation. Traversing through the degrees of freedom and cybernetics, the Authors explain Geodetic reference and prediction algorithms etc. The Global Navigation Satellite System (GNSS) and their function by transliteration, the modern gyroscope and the accelerometer are interesting takeaways.

The next read is on materials. Austenitic structures exhibit close-cubic forms in the Carbon-Temperature phase diagrams for steels. Moving from the construct, Mainak Mukherjee, Jnana Sagar Lokineddi discuss superaustenitic steels, duplex steels etc., with rferences to marine applications. The LR duo explain the compositions, structure, characteristics and applications of the types in use. This will certainly update the knowledge of the practicing marine engineers on the materials front.

Following this, is an article proposing a prediction model based on machine learning. The case in question takes on few physiochemical properties of water and is based on data culled from various other studies and datasets and tries to wed the solution to ballast water. The modelling exercise appears robust, whereas the ballast water relevance remains unanswered, particularly in terms of species count. However, we feature this article, treating it as an exercise in linear and multivariate regression analyses to encourage the researchers' efforts.

The MER Archive from March 1983 has few takeaways... electric fires, CPPs etc. The discussion on wear continues under Lube Matters. We have some electrical knowledge coming in under Competency Corner. In the Heritage Hourglass section, Amruta Talawadekar and Maitre Shah highlight few women achievers in maritime epochs.

Here is the March 2023 issue for your reading pleasure.

Dr Rajoo Balaji
Honorary Editor
editormer@imare.in

MARINE ENGINEERS REVIEW INDIA

JOURNAL OF THE INSTITUTE OF MARINE ENGINEERS (INDIA)

Administration Office
IMEI House
Plot No. 94, Sector - 19, Nerul,
Navi Mumbai 400 706.
Tel. : +91 22 2770 16 64
Fax : +91 22 2771 16 63
E-mail : editormer@imare.in
Website : www.imare.in

Editor
Dr Rajoo Balaji

Editorial Board
Hrishikesh Narasimhan
Dr Sanjeet Kanungo
Chitta Ranjan Dash
Cmde (IN) Bhupesh Tater
Rashmi Tiwari *(Sub-editor)*

Printed, Published and Edited by:
Dr Rajoo Balaji on behalf of The Institute of Marine Engineers (India). Published from 1012 Maker Chambers V, 221 Nariman Point, Mumbai - 400 021, an printed from Corporate Prints, Shop No.1, Three Star Co-op. Hsg. Society, V.P Road, Pendse Nagar, Dombivli (E) - 421 201. District – Thane

Print Version: **Mr Gaurav Kulkarni**

Typesetting & Web designed by:
Kryon publishing (P) Ltd.,
www.kryonpublishing.com

In This Issue

ARTICLES

09 Maturity Assessment of Subsea Navigation and Positioning Systems - Part A
– V. Bala Naga Jyoti, Ramesh Raju, Dr. N. Vedachalam

23 Technological Advancement for the Use of Marine Materials in the Fields of Super Austenitics
– Mainak Mukherjee, Jnana Sagar Lokineddi

28 Prediction Model for the Ballast Marine Water Quality
– Komathy K

COLUMNS

37 Technical Notes
41 Competency Corner
43 Heritage Hourglass
47 Going Astern into MER Archives
50 Election Notification

Cover pictures: **Dr. Jyothi, NIOT, Chennai**

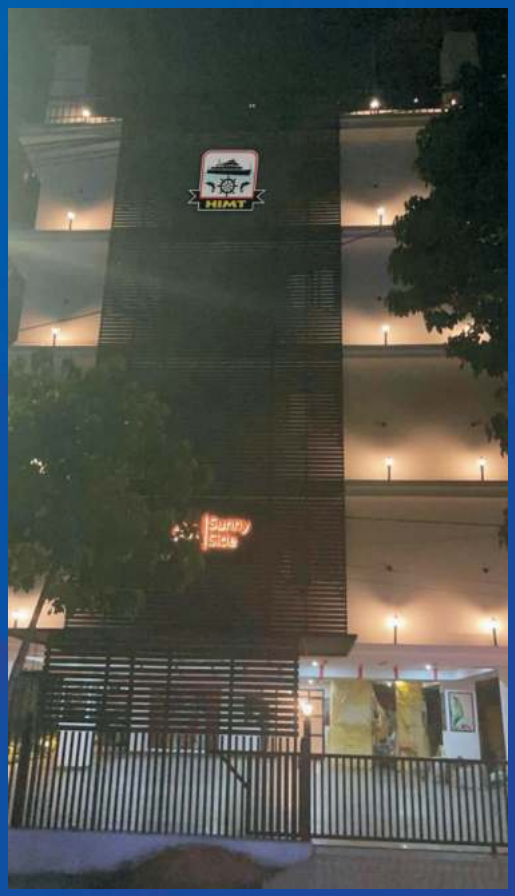

24 YEARS EXCELLENCE IN EDUCATION SINCE 1998

Join the HIMT Family

Required Faculty and Instructors

LOCATION - VIZAG

Instructors

- Bosun/Petty officers/Chief petty officers and above from the seaman branch for Survival Technique course.
- Engine room Apprentice (ERA), Petty officer Mechanical Engineering (POME) and above , NBCD Instructor for fire fighting training.
- Life Guard for swimming pool.

Masters/Chief Engineers

- Tanker Experience is preferred.
- Prior Teaching Experience is preferred.
- Experience in Simulator Training is preferred.
- Chief Engineers competent to teach electrical topics.
- Willingness to take both Competency & Revalidation courses.
- Age below 55 years would be preferred.
- Masters/Chief Engineers with no teaching experience and above 55 years can also apply.

Preference will be given to instructors already teaching PST, PSCRB, AFF, FPFF courses in DG Approved MTI's

Salary

As per Industry Standards

Interested applicants can send a mail to

careers@himtmarine.com

Quality Training | Commitment | Professionalism

MATURITY ASSESSMENT OF SUBSEA NAVIGATION AND POSITIONING SYSTEMS - PART A

V B N Jyothi, R Ramesh, N. Vedachalam

Abstract

Effective manoeuvrability, precise navigation and position determination are the key requirements for effective operations of deep-water and long-endurance autonomous under water vehicles (AUV). The article is published in three parts. This part presents the kinetics and kinematics involved in AUV attitude control when operated in hydrodynamic environments, principles of underwater real-time position determination based on dead-reckoning technique and the technological maturity of the state-of-the-art Inertial Navigation System. Subsequent parts describe the maturity of acoustic sensors/systems, importance of aiding sensor performances and best field application practices in achieving the desired position accuracies. Modelling and simulation case studies presented for seven important scenarios shall help in understanding the intricacies in subsea guidance and navigation system design, identification of mission-specific sensor suite for achieving the desired performance and reliability.

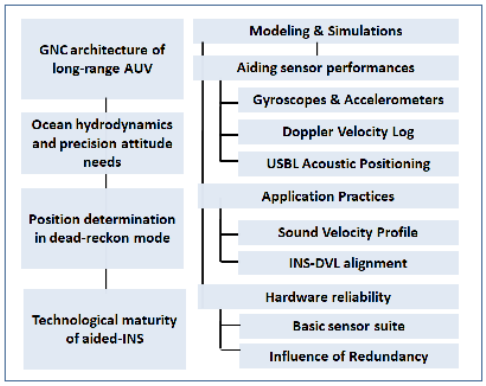

INDEX TERMS: AUV, CONTROL, GUIDANCE, NAVIGATION.

Introduction

Navigation was a major challenge that bedevilled ocean travellers and explorers from the time it was firmly established that the earth is not flat. Ancient sailors watched celestial objects and constellations such as Southern Cross in the Southern hemisphere and Big Dipper in the Northern hemisphere to identify their position. The Pole Star provided a celestial point of reference and became North, opposite end became South, and exactly in-between we placed an artefact called equator.

Compasses, which indicate direction relative to the Earth's magnetic poles, were used for navigation since 11th century. The solar elevation at local noon, measured with a sextant was converted to latitudes, but longitudes presented a big problem until an English carpenter-turned-clockmaker, John Harrison, in 1770s, developed a seagoing, accurate chronometer to determine the difference between local time and Greenwich Mean Time (GMT) to calculate the longitude. Greenwich became longitude zero, which is another artefact.

Since then, technological advancements continued, specifically the commercialisation of the Global Navigation Satellite System (GNSS) in 1978 revolutionised terrestrial

The Pole Star provided a celestial point of reference and became North, opposite end became South, and exactly in-between we placed an artefact called equator

A-INS is one of the important subsystems which helps in precise navigation and positioning of AUVs involved in intelligent, truly-autonomous, long-range and long-endurance subsea missions

navigation with unprecedented position accuracies. However, underwater position determination was a challenge as GNSS electromagnetic signals are attenuated by the saline sea water. Overcoming this challenge, the first use of subsea Acoustic Positioning System (APoS) dates back to 1963 in which a short baseline system was installed on USNS Mizar to guide the bathyscaphe Trieste to the wreckage of American nuclear submarine USS Thresher, and subsequently in 1966 to aid in the search and recovery of a nuclear bomb lost bomber off-Spain. Subsequent demands from the offshore hydrocarbon industry during 1990s matured APoS technologies. During the same period, developments in the Doppler Velocity Log (DVL), depth sensors, inertial measurement sensors and position estimation algorithms led to the realisation of **the underwater Aided-INS (A-INS)**.

A-INS is one of the important subsystems which helps in precise navigation and positioning of AUVs involved in intelligent, truly-autonomous, long-range and long-endurance subsea missions. The world economic forum has highlighted the development of intelligent AUVs as a priority technological requirement for exploring the vast ocean resources and studying climate change. The increased spatio-temporal capabilities for strategic AUVs is evident from the Polar challenge announced by the World Ocean Council involving 2000 km continuous under-ice Polar mission, challenging deep-ocean mineral mining needs that requires precise high resolution mapping of the vast poly-metallic nodule and cobalt crust fields, and the ongoing Seabed 2030 project aimed to create a full global sea floor map by 2030 with a 100m resolution. In order to cope up with the demand, AUVs such as UK NOC's AUTOSUB6000 (with endurance of 70h, operating range of 1000km and capable of undertaking under-ice polar operations) and Kongsberg HUGIN ENDURANCE (with mission ranges up to 2200km and capable of carrying out unsupervised shore-shore operations) with high precision navigation and positioning systems were developed and demonstrated [1][2].

Path planning is the process of finding the course of the points across which the AUV has to travel from the starting location to the target location, represented as North-East-Depth (NED) coordinates

Long-range AUV Guidance, Navigation and Control

The key design considerations for AUV include mission objective, environmental conditions such as currents and density in the operating depth, payloads, communications, navigation, positioning, control, power source and buoyancy mechanisms. The Guidance, Navigation & Control (GNC) system with 3-level architecture used in long-range AUV operating mission objective-based path and trajectory planning algorithms is shown in **Figure. 1**.

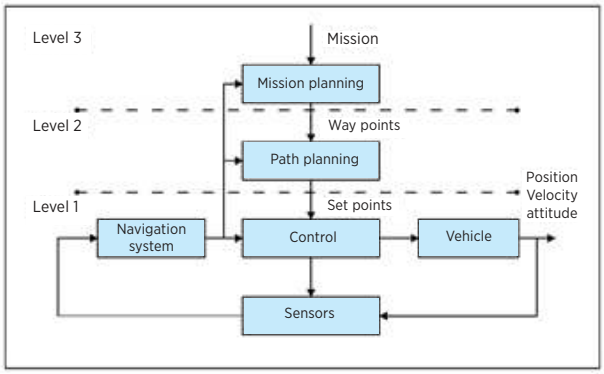

Figure. 1. GNC systems of long-range AUV

With the mission objective as inputs, Level 3Mission Planning Controller (MPC) executes the Trajectory Planning Algorithm (TPA) that determines the way points that serve as inputs for Level-2 Path Planning Controller (PPC).

Path planning is the process of finding the course of the points across which the AUV has to travel from the starting location to the target location, represented as North-East-Depth (NED) coordinates. The Path Planning Algorithm (PPA) provides set points to the AUVLevel-1 controller that takes input from the vehicle navigation systems and other sensor measurements (Level 3 sensors). The underwater path and trajectory planning require due consideration of the dynamic (time-varying) nature of the ocean currents, presence of unknown obstacles and the morphology of the seabed. **The objective anisotropic cost function (executed by the MPC and PPC) is to minimise the travel time/lower energy consumption under the constraints such as on-board energy availability, positioning accuracy, presence of obstacles, utilising/avoiding the prevailing water currents and vehicle manoeuvrability limitations/agility.** The performance of the Level-3 navigation and positioning sensors are the key for precise long range/longer endurance AUV operations [3][4].

Hydrodynamic Environment & AUV Attitude Control

Precise vehicle attitude measurement and control is essential for long-range navigation, carrying out effective seabed mapping and physical robotic

> *The vehicle when operated in the ocean environment experiences hydrodynamic forces (kinetics) which results in the changes in the AUV attitude (kinematics)*

interventions. The vehicle when operated in the ocean environment experiences hydrodynamic forces (kinetics) which results in the changes in the AUV attitude (kinematics). The AUV attitude is represented in 6 degrees of freedom (DoF) include surge, sway and heave in linear orientation, and pitch, roll and heading/yaw (also called Euler angles) in the angular orientation (**Figure. 2**).

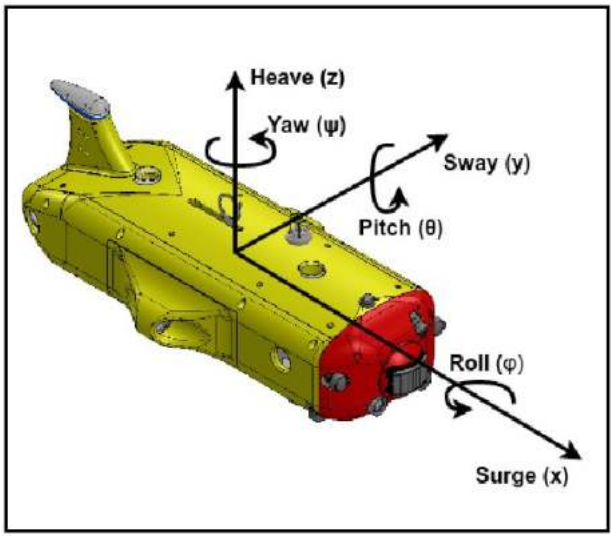

Figure. 2. AUV with six degrees of freedom [3]

The linear forces X, Y and Z, and the angular moments, K M and N, acting on the AUV in 6 DoF is described by below equations of motion (cybernetics notations described in **Table.1**). The term Cybernetics that dates back to 1948, refers to systems and processes involved in automatic control, artificial intelligence, perception and robotics.

$$m[\dot{u} - vr + wq - x_G(q^2 + r^2) + y_G(pq - \dot{r}) + z_G(pr + \dot{q})] = X$$

$$m[\dot{v} - wp + ur - y_G(r^2 + p^2) + z_G(qr - \dot{p}) + x_G(qp + \dot{r})] = Y$$

$$m[\dot{w} - uq + vp - z_G(p^2 + q^2) + x_G(rp - \dot{q}) + y_G(rq + \dot{p})] = Z$$

$$I_x\dot{p} + (I_z - I_y)qr - (\dot{r} + pq)I_{xz} + (r^2 - q^2)I_{yz} + (pr - \dot{q})I_{xy} + m[y_G(\dot{w} - uq + vp) - z_G(\dot{v} - wp + ur)] = K$$

$$I_y\dot{q} + (I_x - I_z)rp - (\dot{p} + qr)I_{xy} + (p^2 - r^2)I_{zx} + (q\dot{p} - \dot{r})I_{yz} + m[z_G(\dot{u} - vr + wq) - x_G(\dot{w} - uq + vp)] = M$$

$$I_z\dot{r} + (I_y - I_x)pq - (\dot{q} + rp)I_{yz} + (q^2 - p^2)I_{xy} + (rq - \dot{p})I_{zx} + m[x_G(\dot{v} - wp + ur) - y_G(\dot{u} - vr + wq)] = N$$

Table. 1. Notations used for AUV Cybernetics

Degree of freedom		Forces & moments	Linear & angular velocities
Translational motion	Surge	X	U
	Sway	Y	V
	Heave	Z	W
Rotational motion	Roll	K	P
	Pitch	M	Q
	Yaw	N	R

In order maintain the AUV attitude amidst the action of external forces and moments in the hydrodynamic environment, equivalent counter forces and moments have to be generated using a combination of propulsion thruster and control surfaces. For characterising the hydrodynamic behaviour, hydrodynamic analysis is carried out (based on scaled-down model tests and by numerical models based on the Navier-Stokes and continuity equations) for determining the propulsion thruster capacity and control surface area required for achieving the desired AUV velocity and manoeuvrability in multiple DoF under various sea states and water currents.

The total force experienced by the AUV is the sum of the drag force and added masses is represented as:

$$T_i(t) = m_i\dot{v}_i(t) + d_{Qi}|v_i(t)|v_i(t) + d_{Li}v(t) + b_i$$

Where i correspond to each DoF, Ti (t) is the net control force, mi is the effective mass which includes vehicle mass and added mass, dQ and dL terms are quadratic and linear components of hydrodynamic drags, bi is the buoyancy. Ti (t), velocity and acceleration are measured with respect to the body frame.

The axial drag force acting on the AUV moving at a constant velocity in the hydrodynamic medium is defined as

$$\text{Drag force} = \frac{1}{2}(C_d\rho AV^2)$$

where C_d is the drag coefficient based on the frontal geometry of the AUV, ρ is the density of sea water medium, A is the exposed frontal area and V is the fluid velocity or advance speed of AUV.

> *The term Cybernetics that dates back to 1948, refers to systems and processes involved in automatic control, artificial intelligence, perception and robotics*

For AUVs, the drag force is the product of the coefficient of the friction drag and the form factor, which is a function of the hull shape. For AUV moving with higher velocities, the thrust requirements increase with square of the velocity. In the case of open frame vehicles (such as ROV and HOV), the added mass is an important component which is due to the effect of forces and moments arising out of the acceleration of the fluid around the vehicle. In case of AUV characterised by slow velocities and modest attitude changes, simplified approaches are followed by neglecting off-diagonal entries, coupled terms, tether dynamics when solving the kinematics in 6 DoF. The automated on-board AUV attitude control (Level-3) systems executes the Proportional (P) or Proportional-Derivative (PD) algorithm with the identified hydrodynamic parameters, counteracts the disturbance by dispatching the desired speed control command to the respective thruster power electronic variable speed controller, adjusting the rudder and fin control surface area [5].

Position Determination in Dead-reckon Mode

In typical deep-ocean AUVs, the Level-3 Navigation and Positioning sensor suite (**Figure. 3**) includes a Global Positioning System (GPS), high-precision Fibre Optic Gyro (FOG) or Ring Laser Gyro (RLG)-based Inertial Navigation Systems (INS) aided by a Doppler Velocity Log (DVL), depth sensor and Acoustic base-line Positioning Systems (APoS).

The AUV navigation system initialised with the position input from the GPS receiver (when at the ocean surface) works in dead- reckoning (DR) mode during underwater mission. In DR mode, based on last known or computed position, the navigational algorithm (operating in L3 real-time controller) estimates the current position based on the inputs from navigation sensor suite. The position is updated from the inputs from the APoS (normally USBL) continuously in real-time [6].

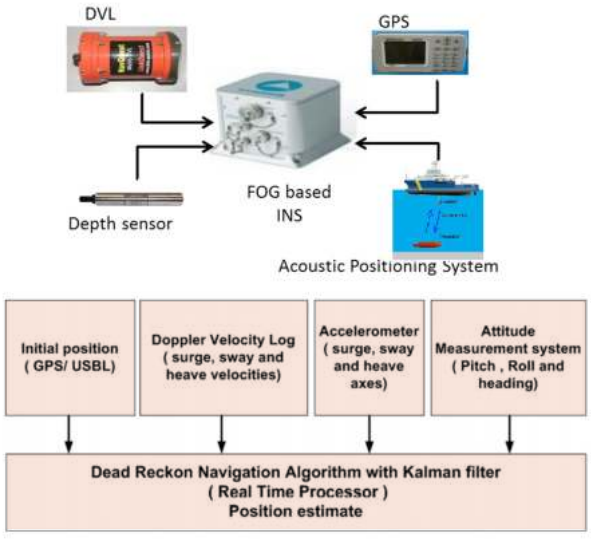

Figure. 3. Architecture of A-INS

The DR algorithm uses the tuned Kalman Filter to estimate the current position along with their uncertainties during aiding sensor outages and measurement delays. The DVL and the accelerometers strapped on the AUV body frame (BF) measures the AUV velocity and accelerations, respectively, in the BF coordinates. In order to compute the position of the AUV with respect to the earth-fixed navigation frame, the measured BF velocity is transformed to Earth Frame (EF) velocity resolved in the North and East directions (**Figure. 4**).

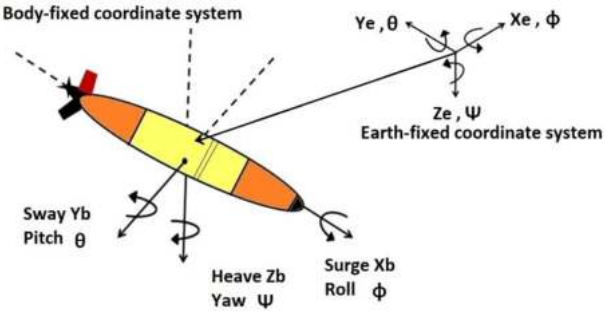

Figure. 4. Body and earth frame representation

The conversion of BF to EF velocity is done using Direct Cosine Matrix (DCM) when the AUV pitch and roll is < 90°, as AUVs are equipped with stabiliser fins to ensure stability in roll axis [3] [6].

Using DCM, the velocity of the AUV in EF is computed using,

$$V_e = C_b^e V_b$$

where, C_b^e is the DCM transformation matrix.

$$C_b^e = \begin{bmatrix} c\psi c\theta & -s\psi c\theta + c\psi s\theta s\phi & s\psi s\phi + c\psi c\phi s\theta \\ s\psi c\theta & c\psi c\phi + s\phi s\theta s\psi & -c\psi s\phi + s\theta s\psi c\phi \\ -s\theta & c\theta s\phi & c\theta c\phi \end{bmatrix}$$

where,s. = sin (.), c. = cos (.) and t. = tan (.), roll (φ), pitch (θ) and Yaw (ψ)or attitude/Euler angles of the AUV and V_b is the BF velocity matrix [V_x, V_y, V_z] and V_e is the EF velocity [V_n, V_e, V_d] matrix.

Typically, quaternion attitude representation is used for underwater vehicles with roll and pitch >90°, as DCM leads to singularity. The below quaternion transformation equation reveals an additional singularity associated with Euler angles, for Cos θ =0,in which w1, w2, w3 are angular measurements in three axis.

$$\begin{pmatrix} \dot{\psi} \\ \dot{\theta} \\ \dot{\phi} \end{pmatrix} = \frac{1}{\cos\theta} \begin{bmatrix} 0 & \sin\phi & \cos\phi \\ 0 & \cos\phi\cos\theta & -\sin\phi\cos\theta \\ \cos\theta & \sin\phi\sin\theta & \cos\phi\sin\theta \end{bmatrix} \begin{pmatrix} \omega_1 \\ \omega_2 \\ \omega_3 \end{pmatrix}$$

The Euler angle matrix C_b measured from the quaterion is

$$C = \begin{bmatrix} q_4^2 + q_1^2 - q_2^2 - q_3^2 & 2(q_1q_2 + q_3q_4) & 2(q_1q_3 - q_2q_4) \\ 2(q_1q_2 - q_3q_4) & q_4^2 - q_1^2 + q_2^2 - q_3^2 & 2(q_2q_3 + q_1q_4) \\ 2(q_1q_3 + q_2q_4) & 2(q_2q_3 - q_1q_4) & q_4^2 - q_1^2 - q_2^2 + q_3^2 \end{bmatrix}$$

where q4 is scalar and q0, q1, q2, and q3 are vectors and are 3-axis rotatonal measurements in yaw, roll and pitch axis.

In case of AUV, with the computed DCM values, the measured BF velocity in the 3 axis Vx, Vy and Vz will be converted to EF velocity V_N, V_E and V_D. The EF-referenced velocity thus obtained is integrated over a sampling duration Δt to get the updated position in geo-coordinates, represented in Latitude and Longitude using equations:

$$\text{Latitude } L = L + \left(\frac{v_N * \Delta t}{R_N}\right)$$

$$\text{Longitude } \lambda = \lambda + \left(\frac{v_E * \Delta t * \sec L}{R_E}\right)$$

where, V_N is the Northing velocity of the AUV in m/s; V_E is the Easting velocity in m/s; R_N is the meridian radius curvature of the Earth, R_E is the transverse radius curvature of the Earth.

$$R_N = \left(\frac{R_E(1-e^2)}{(1-e^2\sin^2 L)^{\frac{3}{2}}}\right)$$

$$R_E = \left(\frac{R_E}{(1-e^2\sin^2 L)^{\frac{1}{2}}}\right)$$

For eccentricity, e, the earth surface is not smooth and cannot be accurately represented by a simple geometrical surface. Nevertheless, it can be approximated by an ellipsoid, a rather simple mathematical surface which is smooth, regular and that fits quite well the geoid since the maximum difference between the geoid and the ellipsoid is <200m.

The most commonly used reference ellipsoid is the World Geodetic System (WGS84) datum featuring coordinates with date and time, is defined and maintained by US National geospatial intelligence agency (**Table. 2** and **Figure. 5**) [7]. With this datum, the position of the AUV is computed with respect to this ellipsoid, by which Latitude, longitude, and elevation are defined.

Table. 2. Earth parameters as per WGS84 standard (ref Figure. 5) [7]

Parameter (Figure.5)	Value	Description
Semi- Major axis, a (R_M)	6378137.0m	Earth ellipsoid semi-major axis
Semi-minor axis, b (R_N)	**63563124.2m**	Earth ellipsoid semi-minor axis
e	**0.0818**	Earth eccentricity
	7.292115 x rad/ sec	Earth rotation rate

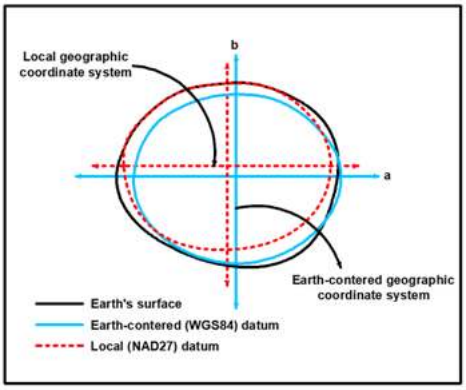

Figure. 5. Geoid of the Earth as WGS 84 standard

The position accuracy of the DVL-aided INS is improved using the APoS aid. The position update interval from APoS to INS (**Figure. 3**) depends on the water depth in which the AUV is operating. With the sound velocity of 1500m/s in water, when the AUV is at 6000m water depth, the frequency of position update rate from APoS is every 4s. Further delays are possible if an acoustic pulse is not received by the AUV transponder due to ocean state and other properties.

Due to the AUV dynamics, there are possibilities that could result in data outages from the DVL to INS that could lead to erroneous position computation. During the period of position unavailability from APoS or inaccurate position inputs computed based on DR principles, the INS rejects the erroneous input (based on the measured and process covariance of the aiding sensor measurement parameters like standard deviation computed with inertial measurements) and estimates the position based on Kalman Predictor Algorithm (KPA) till the residual error is within the acceptable limits.

The KPA is a recursive filter that estimates the internal state of a dynamic system from a time-series of noisy measurements. It uses the current state of the system and the uncertainties involved to predict the next state, without the history of past observations. The most famous use of KPA was in the Apollo-11 lunar module for the moon mission in 1969. Subsequent to this, advanced KPA are being used for various applications, such as Extended Kalman filter (EKF) for non-linearity problems, Unscented Kalman Filter (UKF) for dealing with bias issues, Iterated EKF, Invariant EKF, Particle filter, Ensemble Kalman filter etc., as well as in ML/AI applications [8][9].

The KPA uses the current state (Prior x^_(k-1)) of the system and the measurement uncertainties z_k involved to predict the next state (Posterior x^_k) by calculating the error covariance P_k from the prior error covariance matrix P_k^- which is explained below. The time and measurement update equations are iteratively updated with process, continuously in real-time (**Figure. 6**).

Time Update (Prediction)

Initialisation of the state vector A, B and, H equals to 1. Using the below equations, is the measured value, is assumed to be the Gaussian noise with zero mean and variance.

$$\hat{x}_k^- = A\hat{x}_{k-1} + Bu_k \quad ; z_k = H\hat{x}_k^- + v_k$$

Error covariance initialisation is

$$P_k^- = AP_{k-1}A^T + Q$$

Estimate covariance using the equations

Computation of Kalman Gain K_k

$$K_k = P_k^- H^T (HP_k^- H^T + R)^{-1}$$

Update of estimate via Zk (Zk-)is the residual error which is the difference between the measured value and the prior estimated value, and the error should be minimum which has to be in the acceptable threshold limits. This value determines whether to accept or reject the measured sensor values for posterior position estimate.

$$\hat{x}_k = \hat{x}_k^- + K_k(z_k - H\hat{x}_k^-)$$

Update of error covariance

$$P_k = (I - K_k H) P_k^-$$

Once the correct position input is available from the APoS or DR computations, INS accepts the input. A tuned KPA shall be able to predict the position with better accuracy during the position outage and accept position inputs from reliable sources once available. The position computed from the INS is provided as input to the AUV control system (**Figure. 1**) for further process.

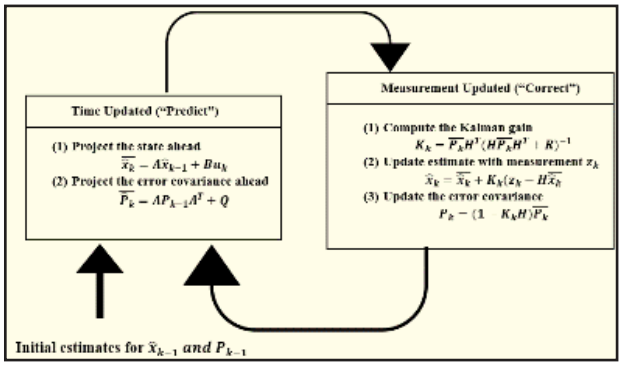

Figure. 6. Principle of Kalman Predictor Algorithm [9]

Technological maturity of A-INS

Understanding inertial sensors performance

The performance of the sensors used in A-INS depends on multiple drift sources including bias instability, random walk behaviour, scale-factor errors and quantisation noise. Sensor noise is described as the short-term variation in the sensor output, such as the peak-to-peak output variation or the standard deviation of the output while the sensor is at rest/static state. It is also defined as a function of frequency using a power spectral density or Fast Fourier Transform (FFT). In these cases, the noise specification will be a noise density that describes the output noise as a function of the bandwidth of the sensors. Such drift parameters are identified and modelled by averaging the measurements for different periods and plotting in a logarithmic graph, called Allan Variance Plot (AVP) with time series data.

The AVP, displayed in a log-log plot (that will give more weight to smaller numbers than larger numbers and accentuate changes) aids to view the noise within a signal over time, segregated into four parts. The parts include the single point noise, improvement from averaging, best case bias and low frequency noise (**Figure. 7**). The sensors inherent drifts and errors are detailed in IEEE-952 standard. The sensor error modelling using AVP is widely carried out for inertial sensors like gyroscope, accelerometers and also for modelling time-series data to identify sensor drifts and noise errors when data is not available from sensor manufacturers [10].

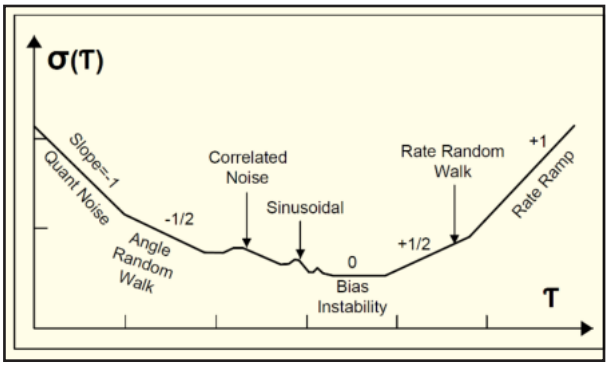

Figure. 7. Log Allan Variance Plot based on IEEE-STD-952[10]

The Angular Random Walk (ARW) describes the average deviation or error that could occur as a result of this noise element, and can be obtained from the AVP (**Figure. 7**) at the 1-sec crossing time. At short averaging times (horizontal axis of the AVP), sensor noise dominates and is given as the -½ slope. The major contributors to random noise are the active elements of the gyro such as the laser diode and photo diode in a FOG, and the silicon or quartz vibrating beam and detection electronics in MEMS gyros. Bias is any non-zero sensor input when the input is zero. A mathematical model is used to calibrate and compensate for the fixed errors such as bias (offset) and input/output scale factor variations.

Thus AVP is intended to estimate stability due to inherent drift and noise processes, and not that of systematic errors such as temperature, shock, or vibration effects. While a gyro's constant bias offset could potentially be calibrated out, bias instability introduces an error that may not be easy to calibrate. Due to bias instability, the longer a gyro/accelerometer operates, the greater it's accumulated rate or position error and hence

there is an accumulated drift that needs to be corrected by periodic initialisation in INS software algorithms.

With the modelled AVP, the key parameters for inertial sensor selection can be done. Hence bias instability is therefore very critical in the I-ANS sensors/subsystems selection criteria. Low bias instability sensors are the key for long-range AUV navigation. The technological trends in the A-INS systems could be understood from the improving trends in sensor performances (**Figure. 8**) [11].

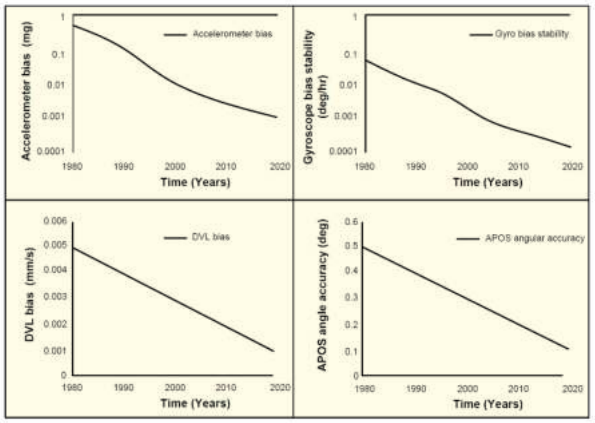

Figure. 8. Performance trends in A-INS sensors/subsystems [11]

Global Navigation Satellite System (GNSS)

As described in **Figure. 3**, the initial position of the AUV is fed from the GNSS receiver in geo-coordinates. Using satellites for navigation began with the US Navy Navigation Satellite System (NNSS)or NAVSAT in 1964 using the TRANSIT satellite system. Subsequently, Global Positioning System (GPS) and GLONASS became operational in 1978 and 1993, respectively. The details of GNSS operated by various countries with a constellation of satellites are summarised in **Table. 3**.

All the positioning application and broadcasting satellites use two carrier frequencies L1 at 1575.42 MHz and L2 at 1227.6 MHz Newer satellites like IRNSS broadcast in L band at 1176 MHz. India's NavIC (Navigation with Indian Constellation) launched in 2013 works in the L5 (1176.45 MHz) and S bands (2492.028MHz) are placed in geo-stationary orbit (GEO) and geosynchronous orbit (GSO). These satellites provide a positioning accuracy of better than 20m over the Indian Ocean region, 1m accuracy over India for public use, and 10cm for authorised users.

Table. 3. GNSS operated by various countries

Name of GNSS	Country	No of satellites	Altitude	Coverage
GPS	USA	24	20400	Global
GLONASS	Russia	24	19100	Global
Galileo	EU	24	23222	Global
BeiDou	China	49	21150	Global
Navic	India	8	36000	Regional
QZSS	Japan	4	42164	Regional

Position of an object on Earth is determined by its Latitude, Longitude on the spheroid and height above the mean sea level (MSL). Navigation satellites work on the principle of trilateration. If at the time of measurement, the instantaneous position of three satellites and the distance of the point of measurement from each of these three satellites are known, then latitude, longitude and height of the location can be determined based on trigonometric relationship. The fourth satellite is required to adjust timing biases.

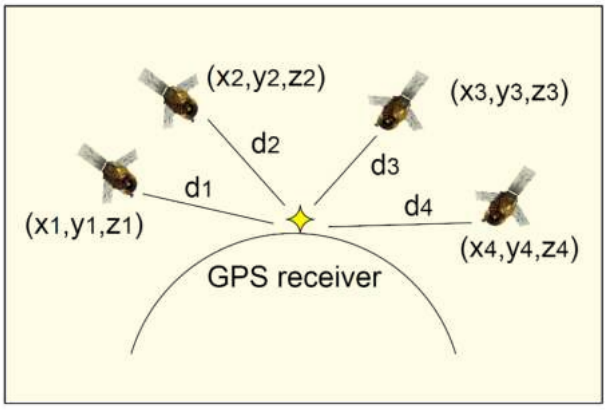

Figure. 9 Position computation of GPS receiver from satellite distance measured using ToF

Since the GPS receiver clock is not perfectly synchronised with the satellite clock, the measured ranges could have errors, and hence called pseudo-ranges. The time offset between the clocks is to be determined to accurately measure the distances. With reference to **Figure. 9**, assuming the distances from the four satellites 1,2 3 and 4 are the exact positions of the satellites, solving the below four equations shall help to eliminate these errors.

$$\sqrt{(x-x_1)^2+(y-y_1)^2+(z-z_1)^2}+ct_B=d_1$$
$$\sqrt{(x-x_2)^2+(y-y_2)^2+(z-z_2)^2}+ct_B=d_2$$
$$\sqrt{(x-x_3)^2+(y-y_3)^2+(z-z_3)^2}+ct_B=d_3$$
$$\sqrt{(x-x_4)^2+(y-y_4)^2+(z-z_4)^2}+ct_B=d_4$$

where c is the speed of light and t_B is the receiver clock offset time. The receiver clock offset is the difference between GPS time and internal receiver time. The

> ***These satellites provide a positioning accuracy of better than 20m over the Indian Ocean region, 1m accuracy over India for public use, and 10cm for authorised users***

unknowns above are x, y, z and t_B. That means if the clocks of the GPS receiver and the satellite were perfectly synchronised, the time offset would be zero.

In pace with the technological developments, differential and relative reference techniques evolved for achieving better position accuracies. With these techniques, differential GPS (DGPS) receivers achieved position accuracies of better than 5m in terrestrial applications, where-in two GPS receiver antennas are placed at a distance of min 2m and the position and heading with true north was computed. Thus using a network of fixed ground-based reference stations to broadcast the difference between the positions indicated by the GPS satellite system and known fixed positions, DGPS provides improved location accuracy in the order of few cm. The DGPS is widely used for terrestrial application where the receivers can get the satellite visualisation periodically. But for the moving vehicles like ships, the visibility of the low earth and middle earth orbits will be poor. Real-time kinematic (RTK) GPS receiver is a type of differential GPS receiver that receives normal signals from GNSS along with position from a fixed station and sends correctional data wirelessly to the moving vehicle. This helps to achieve 1cm positional accuracy.

In the past five years, subsea GPS receivers with antennas are embedded inside hydrostatic pressure-rated and electromagnetically transparent enclosures with pressure-rated cable interfaces (with LED flasher for visibility after surfacing) are available commercially-off-the-shelf (COTS) for use in AUV so that they determine the position when at the ocean surface (**Figure. 10**). The position input could be used by the AUV for correcting the DR position estimates or tracking purposes in conjunction with satellite telemetry. The subsea GPS receivers with high sensitivity of -167dBm(<1pW) can obtain the electromagnetic signal only during surface operations.

Figure. 10. AUV equipped with a subsea GPS receiver

Gyroscope

Gyroscope is an inertial sensor and an important subsystem of INS used for determining the changes in angular DoF (including pitch, heading and roll) computed from rotational rate measurements of the AUV in real-time. Precise INS requires 3-axis gyroscopes with low bias and ARW errors to integrate the measured angular changes over time for obtaining accurate position estimates. Historically, spinning mass gyroscopes that were in operation since 1852 used the properties of the conservation of the kinematic moment of a wheel spinning at high speed. They had the disadvantage of experiencing drift over time due to the inherent friction in the moving parts. Subsequent developments (**Figure. 11**) include the mechanical vibrating gyros based on Coriolis Effect. Hemispherical Resonating Gyros/HRG in 1965, Micro-Electro-Mechanical System/MEMS gyros in 1980s, nuclear magnetic resonance and the dynamically-tuned gyros. Subsequently optical gyroscopes based on Sagnac effect were invented. The Ring Laser Gyroscope (RLG) was demonstrated in 1963 and the Fiber Optic Gyro (FOG) in 1980s. These gyroscopes measure their rotation rate with respect to inertial frame, that includes angular rate of earth rotation around its spinning axis, earth rotation rate around the sun and the angular rate induced by the earth's curvature when the AUV moves over the earth surface [7].

Gyroscope is an inertial sensor and an important subsystem of INS used for determining the changes in angular DoF (including pitch, heading and roll) computed from rotational rate measurements of the AUV in real-time

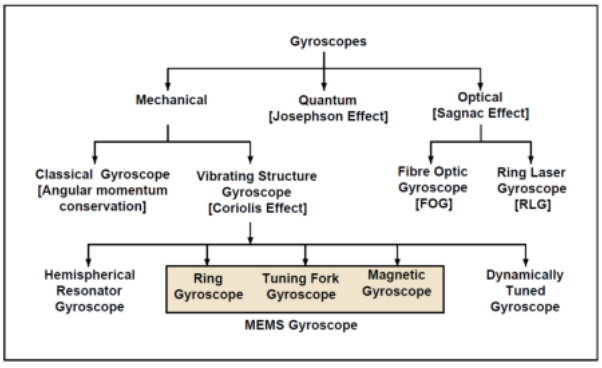

Figure. 11. Classification of gyroscopes

Presently, RLGs had attained full technological maturity, with the latest challenge of "lock-in effect" at very low rotation rates being overcome by mechanical dithering technique, and with this ultimate performance, RLG has taken a very dominant position with 65% and 30% market share in the inertial and tactical grade segments. In order to attain extremely high measurement accuracy (bias stability of 0.0035º/h), RLG needs a larger volume to increase the length of the optical cavity, which makes it expensive. Navigation and strategic grade RLG are manufactured by companies such as Honeywell.

Taking into advantage the rapid technological developments in the low attenuation optical fibre, solid-state light sources and detectors in the telecommunication sector, interference type fibre optic gyroscopes (I-FOG) has emerged as a cost-effective solution for medium

grade applications. Since the demonstration of I-FOG in 1976, > 0.5 million I-FOG axes have been produced in taking an estimated 40% share in tactical grade segment. Developments in polarisation maintaining fibres, super luminescent diodes, optical isolators, fusion splicers and multi-function integrated-optic circuit encourages the use of I-FOG in strategic grade applications where excellent bias stability is required. Further, I-FOG's smaller footprint, light weight, wide dynamic range and faster response have attracted lot of interest. Navigation and strategic grade I-FOG are manufactured by companies such as Ix BLUE [13]. Time transience-related non-reciprocal effect due to ambient temperature variations has significant influence in the bias stability performance of I-FOG. Thermal Finite Element Analysis (FEA) carried out by the Deep Sea Technologies Group in National Institute of Ocean Technology (NIOT) on a 10km long I-FOG sensing coil (**Figure. 12**) of 140µm diameter indicate that even an ambient temperature variation of 0.5º/min could degrade the bias stability performance to tactical grade level (cover picture), while maintaining ambient temperature variations within 0.01º/min is required to attain bias stabilities > 0.001º/h, the performance required for strategic grade applications. Modern I-FOG systems achieve this through quadrupolar winding configuration and precise thermal stabilisation of the sensing coils.

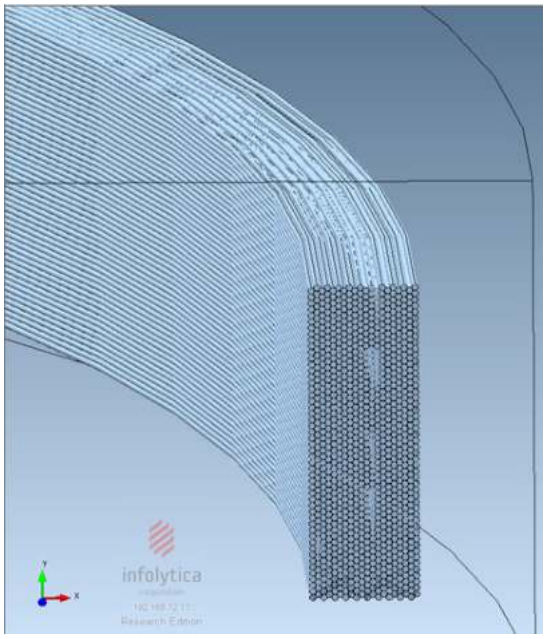

Figure.12. Performance mapping of gyroscopes

The HRG is based on the precession of a standing wave around a vibrating hemispherical form. It uses a thin solid-state hemispherical shell, anchored by a thick stem. The shell is driven to a flexural resonance by electrostatic forces generated by electrodes which are deposited directly onto separate fused-quartz structures that surround the shell. The gyroscopic effect is obtained from the inertial property of the flexural standing waves. It has no moving parts, and can be very compact. The control electronics required to sense and drive the standing waves are sophisticated. HRG with bias stabilities of 0.035º/h are manufactured by Northrop Grumman, Safran and Raytheon Anschütz, etc.

All MEMS gyroscopes (bias stability of ~1º/h) with vibrating element are based on the transfer of energy between two vibration modes caused by the acceleration of Coriolis. The Coriolis acceleration, proportional to the angular velocity, is an apparent acceleration that is observed in a rotating frame of reference. MEMS gyroscopes are manufactured by Northrop Grumman, Silicon sensing, Vectonav etc.

Recently developed magnetic compass-based AHRS have a heading accuracy of 0.25º rms and a resolution of 0.01º. By performing a calibration, the recent TP-TCM identifies the local sources of magnetic distortion and negates their effects from the overall reading to provide an accurate heading. Based on the operating location, they need location-specific calibration [14]. The performance requirements for various grades of gyros are shown in **Table. 4** and **Figure. 13**

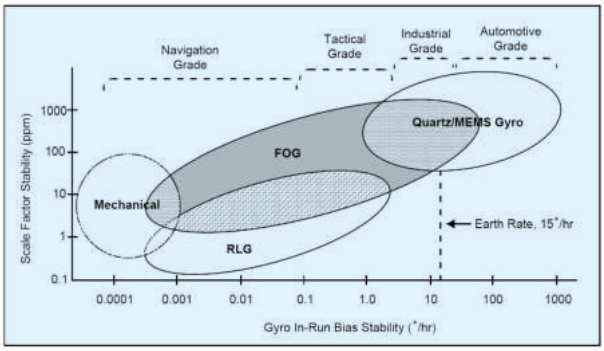

Figure. 13. Performance mapping of gyroscopes

Table. 4. Classification of gyro grades based on performance [15]

Grade	Angular random walk	Bias drift	Scale factor accuracy
Rate	>0.5°	10 - 1000°/h	0.1-1%
Tactical	0.5 - 0.05 °/	1-10°/h	100-1,000 ppm
Intermediate	0.05 - 0.005°/	0.01- 1°/h	10-100 ppm
Inertial	<0.005°/	<0.01°/h	5 ppm
Strategic	<0.003°/	<0.001°/h	1ppm

North-seeing and north-preserving feature are important for navigation-grade gyroscopes that is done using gyro-compassing through sensing the Earth's rotation and gravity vector (**Figure. 13**). The horizontal angle between the observer and north direction is defined as azimuth, α, and measured from north in a clockwise direction, e.g. north is 0° and east is 90°. To determine the azimuth angle without performing physical rotation of a setup, two stationary gyroscopes with the orthogonal sensitive axes are used. Taking into account that cos (α + 90°) = − sin α, the output of these gyroscopes aligned with respect to the gravity [16] [17].

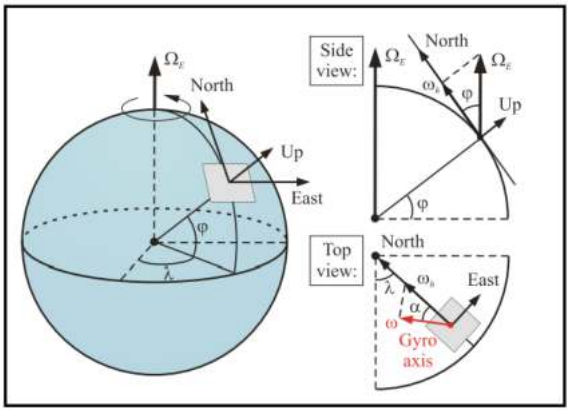

Figure. 14. Gyro-compassing procedure for north-seeking

North-seeking is done using may-tagging and carouseling methods. May-tagging is an azimuth detection method accomplished by the ±180° turning of the gyroscope sensitive axis. It is also commonly referred to as a two-point gyro-compassing, since it mitigates additive bias errors through the differential, two-position azimuth measurement. In carouseling method, continuous rotation of the platform allows identification of the azimuth angle independently of the bias and scale-factor errors (as long as the rate of rotation is faster than the low frequency drift of bias). Specifically, the platform rotation causes a variation of angle between the Earth's rotation axis. The output is maximum when the gyroscope is pointing north and minimum when it is pointing south (**Figure. 14**). The sinusoidal fit to the gyroscope output is performed to extract the phase, which is a measure of heading. Gyro-compassing procedure for 0.15°/h bias gyro, has the capability to seek north with 0.5º accuracy. It has the capability to maintain 0.5º true north accuracy for 3h. A 1°/h bias gyro does not have the capability to seek true north, but can maintain an 0.5º accuracy on true north for 30min (provided that true north has been determined with non-inertial sensors previously).

The typical sensor error model of gyroscope is explained in equation follows considers bias error, bias drift and ARW errors.

$$\omega_o = \omega_i + \partial\omega_{bias}$$

Where,

$$\partial\omega_{bias} = \partial\omega_{biasdrift} + \partial\omega_{turn\text{-}on} + \partial\omega_{random\ walk} \quad (8)$$

ω_i is input angular rotation rate, ω_o is output angular rotation rate, $\partial\omega_{constant}$ is bias error, $\partial\omega_{turn\text{-}on}$ is the bias drift, $\partial\omega_{random\ walk}$ is random walk error which is expressed in ARW (Angular Random Walk in deg/√hour).

$$\frac{d}{dt}\partial\omega_{random\ walk} = w(t)$$

where, w(t) is a zero-mean white noise process with known variance

Accelerometers

Accelerometers are an important subsystem of the INS used for determining the displacement of the AUV in 3 linear DoF (surge, sway and heave axis) in real-time. Precision INS requires accelerometers with low bias errors, as they integrate the measured linear changes for obtaining accurate position estimates. Accelerometers measure acceleration as well as the gravitational field. The strategic grade accelerometers have a resolution of 1µg, stability of <160 µg/year and a scale factor of 300ppm. The performance requirements for various grades of accelerometers are shown in **Table. 5** and **Figure. 15**. Navigation grade accelerometers are manufactured by companies such as Honeywell, Innalabs, etc. [18] [19].

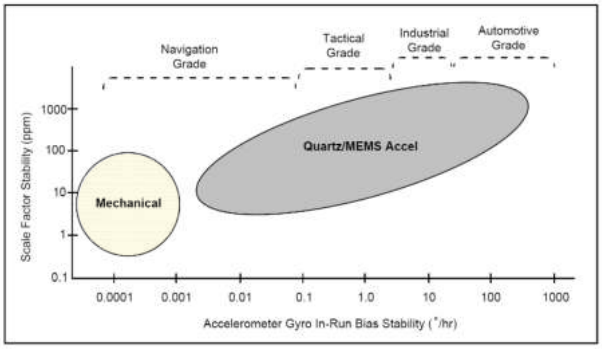

Figure. 15. Performance of accelerometers

Table. 5. Classification of accelerometers based on performance

	Range (g)	Bias stability (mg)	Bandwidth (Hz)	Noise (µg/√Hz)	Scale factor (ppm)
Rate	±100	10	2000	500	2000
Tactical	±60	1	1000	200	500
Intermediate	±50	0.1	500	30	300
Inertial	±30	0.05	100	15	100
Strategic	±10	0.005	75	10	50

Accelerometer error model includes bias instability, scale factor and random walk. The common stochastic error model is,

$$f_o = (1 + S).f_i + b + \eta$$

where, S-Scale factor of accelerometer, b- Bias, f_i-input acceleration, f_o-output acceleration, η-Random bias or random noise.

These sensors data will be provided as inputs to the INS for estimating the velocity and position accurately. The 3-D position data from the A-INS will be fed to the Guidance and Control of AUV for precise attitude control using thrusters and control surfaces.

The next part of the series...

Shall include modelling and simulation cases using Bellhop software and MATLAB to understand the importance of sensor characteristics in achieving the desired Aided-Inertial Navigation System performances

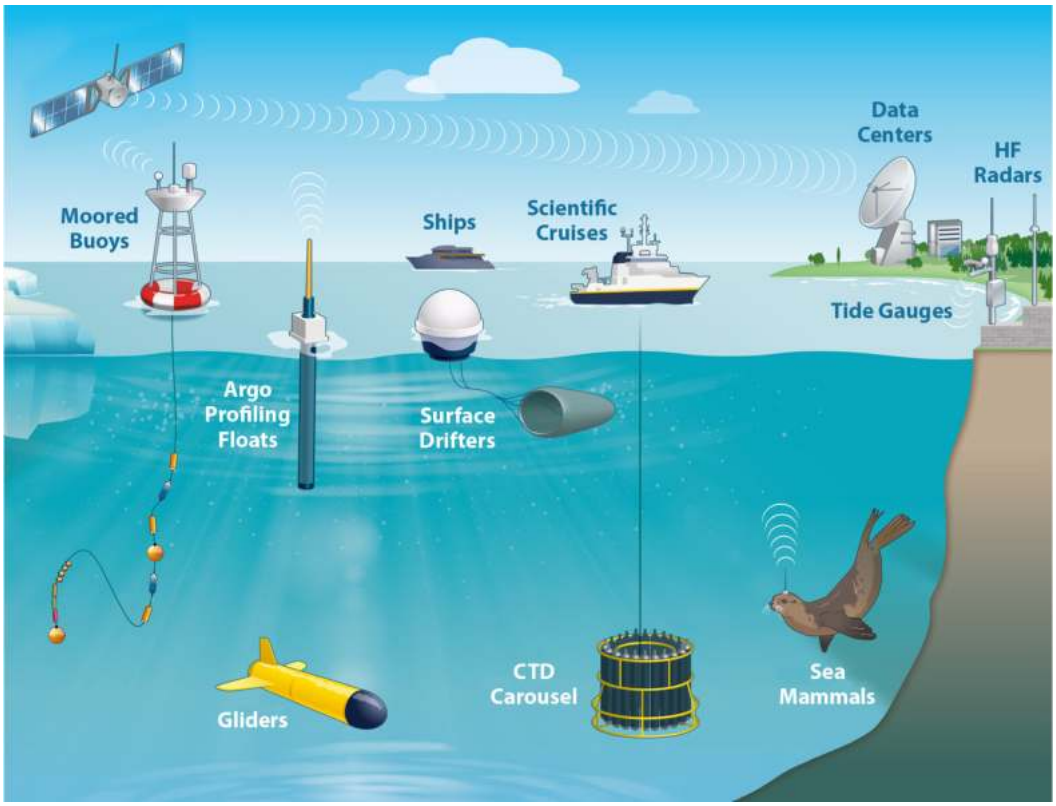

and best field application practices in achieving desired position accuracies.

Modelling and simulation case studies shall be presented for the following practical scenarios described in below Table. The next part also features a hardware reliability analysis on the A-INS subsystems carried out using probabilistic reliability modelling and simulations software TOTAL-GRIF by which the Mean Time to Fail (MTTF) period for various configurations are identified.

Case	Description
A	Performance assessment of APoS in various water depths and sea states based on Bellhop modelling and simulations
B	Importance of aiding sensor performance (with INS and DVL) and without APoS in AUV Nav & Pos
C	Position error when descend/ascend of AUV without APoS from 6000m water depth in spiralling mode in the presence of ambient water currents
D	Influence of AUV mounted gyroscope-DVL misalignment
E	Positioning error without sound velocity profile inputs to APoS
F	Relative position error of the AUV without ship attitude real-time correction
G	Position error with APoS aid with varying transceiver beam angle coverage

ABBREVIATIONS

AHRS	Attitude Heading Reference system
AI	Artificial Intelligence
A-INS	Aided Inertial Navigation System
APoS	Acoustic Positioning System
ARW	Angular Random Walk
AUV	Autonomous Underwater Vehicle
AVP	Allan Variance Plot
BF	Body Frame
BDS	BeiDou Navigation Satellite System
COTS	Commercial Off The Shelf
DCM	Direction Cosine Matrix
DOA	Direction of Arrival
DoF	Degree of Freedom
DGPS	Differential Global Positioning System
DSP	Digital Signal processing
DR	Dead Reckoning
DVL	Doppler Velocity Log
EF	Earth Frame
EKF	Extended Kalman Filter
FFT	Fast Fourier Transform
FOG	Fiber Optic Gyroscope
GC	Gyro Compass
GEO	Geostationary Earth Orbit
GPS	Global Positioning System
GMT	Greenwich Mean Time
GNC	Guidance Navigation Control

GNSS	Global Navigation Satellite System
GSO	Geo Synchronous Earth Orbit
HOV	Human Occupied Vehicle
HRG	Hemispherical Resonant Gyroscope
IEEE	Institute of Electrical and Electronics Engineers
IMU	Inertial Measurement Unit
I-FOG	Interference Fiber Optic Gyroscope
INS	Inertial Navigation System
IRNSS	ISRO Regional Navigation Satellite System
ISRO	Indian Space Research Organisation
KPA	Kalman Predicator Algorithm
LBL	Long Baseline Line
LED	Light Emitting Diode
LEO	Low Earth Orbit
LEOS	Laboratory for Electro Optics System
MEO	Middle Earth Orbit
MEMS	Micro Electro Mechanical Systems
ML	Machine Learning
MHz	Mega Hertz
MPC	Mission Planning Control
NAVIC	Navigation with Indian Constellation
NavSat	Navigation

NED	North East Depth
NOC	National Oceanographic Centre
NNSS	Navy Navigation Satellite System
PD	Proportional Derivative
PPA	Path Planning Algorithm
PPC	Path Planning Controller
pW	Pico Watts
QZSS	Quasi Zenith Satellite System
RLG	Ring Laser Gyroscope
ROV	Remotely Operable Vehicle
RTK	Real-Time Kinetic
SVP	Sound Velocity Profile
TDOA	Time difference of arrival
TOF	Time of Flight
UK	United Kingdom
USBL	Ultrashort baseline
US	United States
VRW	Velocity Random Walk
WGS	World Geodetic Standard

ACKNOWLEDGEMENTS

We thank the Ministry of Earth Sciences, Govt. of India for motivating this study.

REFERENCES

1. Wynn, Russell B., Veerle AI Huvenne, Timothy P. Le Bas, Bramley J. Murton, Douglas P. Connelly, Brian J. Bett, Henry A. Ruhl et al. "Autonomous Underwater Vehicles (AUVs): Their past, present and future contributions to the advancement of marine geoscience." *Marine geology* 352 (2014): 451-468.
2. N. Vedachalam, R Ramesh, V Bala Naga Jyothi, V Doss Prakash, G A Ramadass, 2018, Autonomous Underwater Vehicles - Challenging developments and technological maturity towards strategic swarm robotics systems, Taylor & Francis Journal of Marine Georesources & Geotechnology, https://doi.org/10.1080/1064119X.2018.1453567.
3. Fossen, Thor I. "Marine control systems–guidance. navigation, and control of ships, rigs and underwater vehicles." Marine Cybernetics, Trondheim, Norway, Org. Number NO 985 195 005 MVA, www. marine cybernetics. com, ISBN: 82 92356 00 2 (2002).
4. Jalving, Bjorn, Kenneth Gade, Ove Kent Hagen, and KarsteinVestgard. "A toolbox of aiding techniques for the HUGIN AUV integrated inertial navigation system." In *Oceans 2003. Celebrating the Past... Teaming Toward the Future (IEEE Cat. No. 03CH37492)*, vol. 2, pp. 1146-1153. IEEE, 2003.
5. N. Vedachalam, Technologies for next generation autonomous underwater vehicles, Marine Engineers Review (India), Volume 15, Issue 8, July 2021.
6. Fanelli, Francesco. "Development and testing of navigation algorithms for autonomous underwater vehicles." (2020): 1-xix.
7. Word Geodetic System WGS84, https://gisgeography.com/wgs84-world-geodetic-system/.
8. Narayanswamy, Vedachalam, Bala Naga Jyothi Vandavasi, Doss Prakash Vittal, Ramesh Raju, and Vadivelan Arumugam. "Overload Protection of Marine Power Generators Using Supervised Machine Learning-Based Kalman Predictor Algorithm." *Marine Technology Society Journal* 55, no. 5 (2021): 109-115.
9. R. Ramesh, V. Bala Naga Jyothi, N. Vedachalam, G.A. Ramadass and M.A. Atmanand, 2016, Development and performance validation of a navigation system for an underwater vehicle, The Journal of Navigation, Vol.69, pp:1097-1113.
10. Allan Variance Plot, IEEE-STD-952, IEEE Standard Specification Format Guide and Test Procedure for Single-Axis Interferometric Fiber Optic Gyros
11. VBN Jyothi, R Ramesh, N. Vedachalam, G A Ramadass, Assessment of the Technological Maturity of Manned Submersible Navigation Positioning Systems, Marine, Volume 55, Number 5, September/ October 2021, pp. 129-137(9).
12. GPS Maral, Gerard, Michel Bousquet, and Zhili Sun. Satellite communications systems: systems, techniques and technology. John Wiley & Sons, 2020.
13. Gidugu Ananda Ramadass, Narayananswamy Vedachalam, Arunachalam Umapathy, Raju Ramesh, Vandavasi Balanagajyothi, 2017, Finite element analysis of the influence of ambient temperature variations on the performance of fibre optic gyroscope sensing coils, Marine Technology Society Journal, Vol.51, Number 1, January/February 2017, pp. 16-22(7).
14. Digital Compass and Attitude & Heading Reference System (*AHRS*), www.pnicorp.com
15. Lefevre, Herve C. *The fibre-optic gyroscope*. Artech house, 2022.
16. Hua Sun, Fang Zhang and Haojun Li, Design and implementation of fibre optic gyroscope north seeker, IEEE proceedings, 2010, International Conference on Mechatronics and Automation.
17. Zhu Zhou et al. Modified dynamic north finding scheme with a fibre optic gyroscope, IEEE Photonics Journal, Vol.10, Number 2, April 2018.
18. Titterton, David, John L. Weston, and John Weston. Strap down inertial navigation technology. Vol. 17. IET, 2004.
19. Beitia, J. "Miniature high-performance Quartz accelerometer for High-Dynamic, precision guided systems." In 2017 DGON Inertial Sensors and Systems (ISS), pp. 1-13. IEEE, 2017.

About the authors

Mrs. V. Bala Naga Jyoti is Scientist-E at National Institute of Ocean Technology, India. She is a lead electronics engineer for the development of navigation and positioning systems for India's indigenously-developed deep-water manned scientific submarine Matsya6000 and unmanned remotely operated vehicles. Prior to NIOT, she was working as a Scientist/ Senior Engineer in Indian Space Research Organization (ISRO) involved in the control and automation of Cryogenic Propellant Systems of Geo-Stationary Launch Vehicles (GSLV) and Attitude On-Orbit Control Systems of geo-stationary satellites. Presently she is pursuing doctoral degree in the development of machine-learning/artificial intelligence-based homing guidance systems for autonomous underwater vehicles using electromagnetic, optical and hybrid techniques aided by sensor fusion. She has published more than 30 papers in indexed journals, international and national conferences. She is a member of Ocean Society of India (OSI), Marine Technology Society (MTS) and IEEE.

Email: nagajyothi@niot.res.in

Mr. Ramesh Raju is Scientist- E at National Institute of Ocean Technology, Chennai, India. He is a lead electronics engineer for India's first indigenously-developed deep-water scientific manned submersible Matsya6000. He had designed, developed, and tested control hardware and software for shallow water and deep water Remotely Operated Vehicles (ROV)rated up to depth of 6000m. He is an ROV pilot for NIOT-developed ROVs and operated up to 5289m. He has participated in 34thIndian Scientific Expedition to Antarctica for shallow water cum polar ROV operation and piloted the ROV at Lake and New Indian barrier in East Antarctica. His experience includes data telemetry and control systems for unmanned and manned underwater vehicles, instrumentation and automation for the compact disc industry, and calibration and testing of test and measuring instruments. He is a recipient of the National Geoscience award 2010 and National societal innovation award 2018for the development and usage of underwater robotic vehicles. He has published more than 40 papers in indexed journals, international and national conferences.

Email: rramesh@niot.res.in

Dr. N. Vedachalam is currently Scientist G in Deep Sea Technologies division of National Institute of Ocean Technology (NIOT), Ministry of Earth Sciences, India. He is the technical lead for India's first indigenously-developed deep-water manned scientific submarine MATSYA 6000. He holds a Bachelor's degree in Electrical and Electronics engineering from Coimbatore Institute of Technology (1995) and PhD in Techno-economics of marine gas hydrates from College of Engineering - Anna University, India. His 27 years of experience include industrial power, process, offshore and subsea domains at Aditya Birla group, General Electric & Alstom Power Conversion in France. Technical exposure includes development of multi-megawatt subsea power and control systems for Ormen Lange subsea compression pilot; Ocean Thermal Energy Conversion and wave energy systems; subsea renewable power grids; unmanned and manned underwater vehicles; ocean observation technologies and industrial systems. His research interests include energy, subsea robotics and reliability. He has more than 100 publications in indexed journals, holds an international and two national patents in subsea robotics and subsea processing. He is a recipient of the national meritorious invention award in 2019 for the development and usage of underwater robotic vehicles. He is a member of Indian Naval Research Board, member of Bureau of Indian Standards and was the Secretary of IEEE OES - India Chapter. He is a regular contributor to MER.

Email: veda1973@gmail.com

TECHNOLOGICAL ADVANCEMENT FOR THE USE OF MARINE MATERIALS IN THE FIELDS OF SUPER AUSTENITICS

Mainak Mukherjee,
Jnana Sagar Lokineddi

A super austenitic stainless steel is considered to be one with a Pitting Resistance Equivalent Number (PREN) greater than 40. This is usually attributed to alloys with high additions of molybdenum, typically 6% or greater. Austenitic stainless steels are the most used family of stainless steels in general engineering applications. Most of the popular grades of Superaustenitics are UNS S31254 (W. Nr 1.4547); UNS S32654 (W. Nr 1.4652); UNS N08028 (W. Nr 1.4563).

Duplex stainless steels belong to the stainless steels family and are characterised by high chromium (Cr, 19 % to 30 %) and molybdenum (Mo, up to 5 %) and lower Nickel (Ni) contents than Austenitic stainless steels and identified by a dual phase microstructure. They have a well-balanced two-phase structure. Duplex grades account for less than 3 % of global stainless-steel production, however with a strong growth rate. They are most used when a combination of high mechanical strength and high corrosion resistance is required. Main Specification for Duplex stainless steel is UNS S31803 ASTM, UNS S32205 (W. Nr 1.4462). Most popular Duplex stainless steel is UNS S31803 and super duplex is UNS S32750 (W. Nr 1.4410).

Grade 630 stainless steels are martensitic stainless steels that are precipitation hardened to achieve excellent mechanical properties. These steels achieve high strength and hardness following heat treatment. This Grade is also commonly referred to as Grade 17-4PH. One of the key benefits of this Grade is that it is available in solution treated conditions, at which they can be easily machined and age-hardened to attain high strength.

This paper looks at the study of technological advancement for the use of Marine materials in the fields of Superaustenitics, Duplex, Super Duplex and 17-4PH Martensitic precipitation hardened Stainless steel.

KEY WORDS: Super Austenitic stainless steel; Duplex and Super Duplex Stainless Steel, 17-4PH Martensitic precipitation hardened Stainless steel; Stress corrosion cracking, Pitting Corrosion cracking; Crevice corrosion cracking and Pitting Resistance Equivalent Number (PREN).

1. INTRODUCTION

STAINLESS STEELS are iron-base alloys which contain about 12% of Chromium, the amount needed to prevent the formation of rust in unpolluted atmospheres. This is the reason for the name 'stainless.' Few stainless steels contain more than 30% Cr or less than 50% iron. They achieve their stainless characteristics through the formation of an invisible and adherent chromium-rich oxide film. This oxide forms and heals itself in the presence of oxygen. Other elements added to improve characteristics include nickel, manganese, molybdenum, copper, titanium, silicon, niobium, aluminum, sulphur, and

selenium. Carbon is normally present in amounts ranging from less than 0.03% to over 1.0% in certain grades.

With specific restrictions in certain types, the stainless steels can be shaped and fabricated in conventional ways. They are produced in cast, powder metallurgy, and wrought forms.

Available wrought product forms include plate, forgings, sheet, strip, foil, bar, wire, semi-finished products (blooms, billets, and slabs), and pipe and tubing. **Cold rolled flat products (sheet, strip, and plate) account for more than 60% of stainless-steel product forms.**

Stainless steels are used in a wide variety of applications. Most of the structural applications occur in the chemical and power engineering industries, which account for more than a third of the market for stainless steel products (see the following table). These applications include an extremely diversified range of uses, including nuclear reactor vessels, heat exchangers, oil industry tubulars, components for chemical processing and pressure vessels, furnace parts, and boilers used in fossil fuel electric power plants.

Historically, stainless steels have been classified by microstructure and are described as austenitic, martensitic, ferritic, duplex (Austenitic plus ferritic).

In addition, a fifth family, the precipitation-harden able (PH) stainless steels, is based on the type of heat treatment used rather than the microstructure.

This paper looks at the study of technological advancement for the use of Marine materials in the fields of Superaustenitics, Duplex, Super Duplex and 17-4PH Martensitic precipitation hardened Stainless steel.

2. SUPER AUSTENITIC STAINLESS STEEL

A super austenitic stainless steel is considered to be one with a Pitting Resistance Equivalent Number (PREN) greater than 40. This is usually attributed to alloys with high additions of molybdenum, typically 6% or greater. Austenitic stainless steels are the most used family of stainless steels in general engineering applications. The 3xx series are relatively straightforward to fabricate and weld, possess excellent toughness across a wide range of temperatures, and reasonable levels of corrosion resistance. By increasing the amount of chromium and molybdenum present in Superaustenitics, it is possible to significantly increase the resistance to pitting corrosion. However, to retain the favourable mechanical and physical properties of Superaustenitics stainless steel, the nickel content must also be increased.

PREN shall be calculated by the following formula:
PREN=%Cr+3.3x(%Mo) + 16x(%N).

This formula is applicable with Superaustenitics and also for duplex and super duplex stainless steels.

PREN for Superaustenitics shall be greater than 40, for duplex stainless steel it is greater than 35 and super duplex stainless steel it is greater than 40.

Most popular grades of Superaustenitics are UNS S31254 (W. Nr 1.4547); UNS S32654 (W. Nr 1.4652) and UNS N08028 (W. Nr 1.4563).

For UNS S31254 (W. Nr 1.4547) is the most common so called Super Austenitic Stainless steel, the Molybdenum content helps to achieve a PREN of 43 compared with just 25 of Austenitic Stainless steel with grade 316L.

“Historically, stainless steels have been classified by microstructure and are described as austenitic, martensitic, ferritic, duplex (Austenitic plus ferritic).”

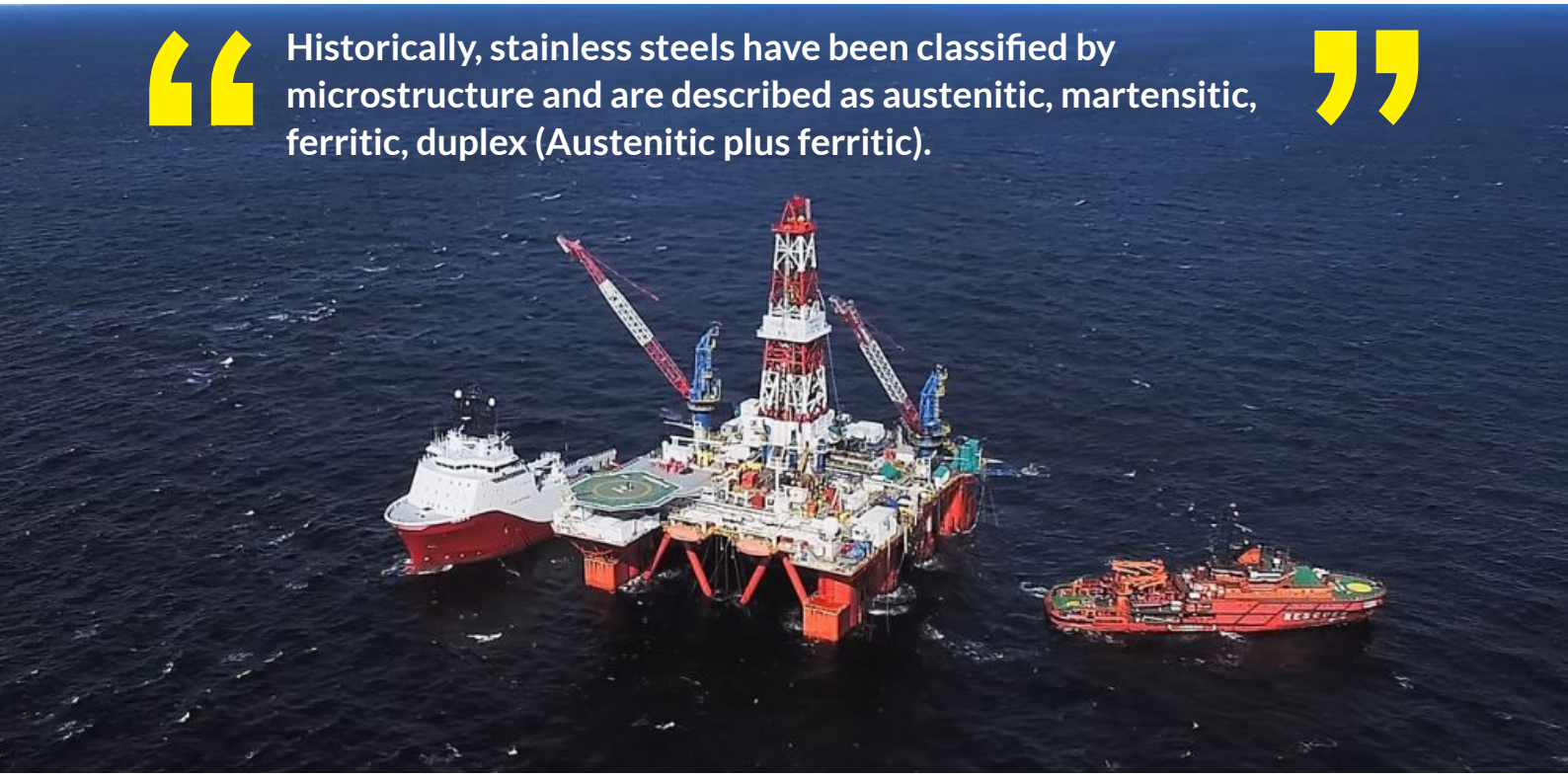

For UNS S32654 (W. Nr 1.4652) contents nearly 8% Molybdenum which pushes its PREN to 54 which will have best pitting corrosion resistance.

A typical Chemical composition of grade UNS S31254 (W. Nr 1.4547) is given below.

C-0.02%max., Cr-19.5 to 20.5%, Mn-1%max, Mo-6 to 6.5%, Ni-17.5 to 18.5%, N-0.18 to 0.25%, P-0.03%max., S-0.01%max. and Si-0.8%max.

UNS N08354, ASME Code 2585-1 is a Superaustenitics stainless steel with PREN greater than 54 and excellent corrosion resistant in various environments. The high chromium, molybdenum and nitrogen contents provide high resistance to crevice and pitting corrosion in oxidising chloride environments while the high nickel content enhances resistance to stress corrosion cracking. The corrosion resistance of N08354 exceeds the conventional 6 Mo super austenitic stainless steels because of containing 7.5% Mo.

UNS N08028 (W. Nr 1.4563) (Alloy 28) is a Nickel – Iron – Chromium alloy with additions of Mo and Cu. It has excellent resistance to both reducing and oxidising acids to stress corrosion cracking and to localise attack such as pitting and crevice corrosion (PREN of 39). The alloy is especially resistant to sulphuric acid and phosphoric acid.

This alloy is used for Chemical processing, oil and gas well piping, Cargo piping systems of Oil and Chemical tankers, pollution control equipment in marine industry and nuclear fuel reprocessing. Alloy 28 is available in instrument tube, precision tube and hydraulic tube. (Ref. 3).

Some of the other marine applications of above Superaustenitics are submerged items like pipelines and grills for oil, sewage and water, risers for oil platforms, heat exchangers for Ships and coastal power plants, equipment attached to hulls of boats and Ships, pumps, winches and Transverse and longitudinal bulkheads for Cargo tanks in Oil and Chemical Tankers.

3. DUPLEX STAINLESS STEEL

Duplex stainless steels belong to the stainless steels family and are characterised by high chromium (Cr, 19% to 30%) and molybdenum (Mo, up to 5 %) and lower Nickel (Ni) contents than Austenitic stainless steels and identified by a dual phase microstructure. They have a well-balanced two-phase structure. The two phases in their microstructure consist of grains of ferrite and austenite. The microstructure contains roughly 50% austenite and 50% ferrite. In practicality we get around 42 to 45% Ferrite and the remaining is Austenite.

Besides the phase balance, there is a second major concern with Duplex stainless steel and their chemical composition i.e., the formation of detrimental intermetallic phases at elevated temperatures. Sigma and Chi phases form in duplex stainless steel and precipitate preferentially at the grain boundaries in the ferrite in

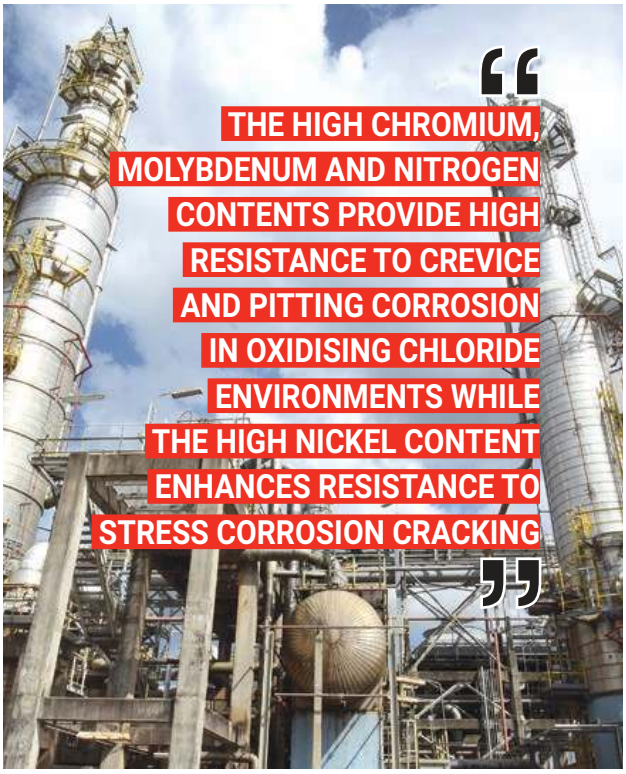

the temperature range of 450C to 1000C. The addition of Nitrogen significantly avoids the formation of these phases. Therefore, it is necessary that significant Nitrogen is present in Duplex stainless steel specifications. Care must be taken during solution annealing heat treatment to avoid sigma and Chi phases significantly. High content of Chromium and Molybdenum improves intergranular and pitting corrosion resistance, respectively.

The two-phase microstructure guarantees higher resistance to pitting and stress corrosion cracking in comparison with conventional 300 series stainless steel.

Duplex grades account for less than 3% of global stainless-steel production, however with a strong growth rate. They are most used when a combination of high mechanical strength and high corrosion resistance is required.

Main Specification for Duplex stainless steel is UNS S31803, UNS S32205 (W. Nr 1.4462) and the use of these grades accounting for more than 80% of Duplex use.

Most popular Super duplex stainless steel grades with 25-26% Chromium and increased Molybdenum and Nitrogen such as UNS S32750, UNS S32760 and UNS S32550 where PREN is greater than 40.

UNS S31803 and UNS S32750 grades are used as Marine grades.

Hyper duplex refers to duplex grades with a PREN greater than 48 and examples are UNS S32707 and UNS S33207. (Ref. 6 & 7)

Ferrite/austenite phase balance in the microstructure can be predicted by the following equations.

Some of the marine applications of above Duplex & super duplex stainless steels are pressure vessels and storage tanks, hot water tanks, hot water boilers, Asphalt hauling tanker, Flue gas desulphurisation plants, Desalination plants (Fresh water generators), processing plants and Oil and gas applications

Cr(eq) = %Cr+1.73 %Si + 0.88 %Mo

Ni(eq) = %Ni + 24.55 %C + 21.75 %N + 0.4 %Cu

% Ferrite = -20.93 + 4.01 Cr(eq) – 5.6 Ni(eq) + 0.016 T

where T (in deg. C) is the Solution annealing temperature ranging from 1050C to 1150C and the elemental compositions are in weight %.

The attractive combination of high strength, wide range of corrosion resistance, moderate weldability would seem to offer great potential for duplex stainless steels.

Some of the marine applications of above Duplex & super duplex stainless steels are pressure vessels and storage tanks, hot water tanks, hot water boilers, Asphalt hauling tanker, Flue gas desulphurisation plants, Desalination plants (Fresh water generators), processing plants and Oil and gas applications.

4. (17-4PH) MARTENSITIC PRECIPITATION HARDENED STAINLESS STEEL

Grade 630 stainless steels are martensitic stainless steels that are precipitation hardened to achieve excellent mechanical properties. These steels achieve high strength and hardness following heat treatment. This Grade is also commonly referred to as Grade 17-4PH.

17-4 PH, or simply 17-4; also known as UNS S17400 is a Grade of martensitic precipitation hardened stainless steel. It contains approximately 15–17.5% chromium and 3–5% nickel, as well as 3–5% copper. This Grade is called UNS S17400 Type 630/ASTM A564/W. Nr 1.4542. The name comes from the chemical makeup which is approximately 17% chromium (Avg. of 15 to 17.5%) and 4% Nickel (Avg. of 3 to 5%).

One of the key benefits of this Grade is that it is available in solution treated conditions, at which they can be easily machined and age-hardened to attain high strength. The age hardening treatment of Grade 630 is carried out at low temperatures, to avoid significant distortion. Therefore, this Grade is used for applications such as the manufacture of long shafts that do not require re-straightening after heat treatment.

This grade can be solution treated by heating material to 1040C minimum, soaking for 0.5hrs air cooled to room temperature. After this solution treatment age hardening table is to be followed.

Table 1: Typical mechanical properties of grade 630 steels achieved after solution treating.

Condition	Temp (Deg. C)	Time (h)	Typical Hardness HRC	Typical Tensile Strength (MPa)
A	Solution Annealing	-	36	1100
H900	482	1	44	Above 1320
H925	496	4	42	1170-1320
H1025	552	4	38	1070-1220
H1075	580	4	36	1000-1150
H1100	593	4	35	970-1120
H1150	621	4	33	930-1080

Table 1 shows the typical mechanical properties of grade 630 steels after solution treatment and age hardening.

H stands for age hardening. 900 is the temperature in Fahrenheit. Hardness is in Rockwell which decreases when the soaking temperature is increases and tensile strength also has been decreased, respectively. Therefore, Grade 630 stainless steels are age-hardened at low temperatures to achieve the intended mechanical properties. (Ref. 13 &14).

Some of the Marine applications of above 17-4 PH is deck components for boats and Ships like deck eyes, brackets for Anchor ropes, housings for equipment's, shackles, handrails, Engine components, High strength boat propeller shafts, valves, and gears.

5. CONCLUSIONS

To conclude we have discussed about the use of marine materials in the fields of Superaustenitics, Duplex, Super Duplex and 17-4PH Martensitic precipitation hardened Stainless steel.

Superaustenitics has PREN more than 40% and Mo is minimum 6% and these materials are used in predominant pitting corrosion and crevice corrosion environments.

Duplex and super duplex stainless steels contains roughly 50% Ferrite and 50% Austenite, PREN greater than 40 with two-phase microstructure which guarantees higher resistance to pitting and stress corrosion cracking. This grade can be used where there is a chance of pitting corrosion like Sour gas, desalination plants, etc.

About the Author

Mainak Mukherjee is a Senior Metallurgical Consultant and Lead Metallurgical and Welding Specialist with LRQA Inspection services India LLP.

Jnana Sagar Lokineddi is a Surveyor with Lloyd's Register Marine and Offshore India LLP.

Email: sagar.lokineddi@lr.org

It is quite evident that 17-4PH stainless steel is the most used type of PH stainless steels. It has an ideal combination of corrosion resistance, good mechanical properties at high temperature and high yield strength. This combination makes it a suitable alloy for cost effectiveness and for many applications.

REFERENCES

1) Handbook of Stainless steel, McGraw Hill Publication, D. Peckner and I.M. Bernstein.
2) Metals Handbook, 9th Ed. Vol.4, ASM
3) www.ispatguru.com for duplex and super duplex stainless steels.
4) Duplex and Super Duplex by Cadence Engineering Services Ltd. U.K
5) ASME Sec. II Part A: 2021: SA789 UNS S31803, UNS S32205, UNS S32750, UNS S32760, SA 790 UNS S31803, UNS S32205, UNS S32750 and UNS S32760.
6) ASME Sec. II Part A: 2021: SA240 UNS S31254, UNS S32654, SA479: UNS S31254; SA312: UNS S31254, UNS S32654, SA269: UNS S31254. SA182 F44.
7) Analysis of Super Duplex Stainless Steel Properties as an Austenite-Ferrite Composite; Fady M. Elsabbagh, Ahmed El-Sabbagh, Rawia M. Hamouda, Mohamed A. Taha. Published 21 December 2015.
8) Duplex Stainless Steels-An overview; Sunil Dayarambhai Kahar; April 2017International Journal of Engineering Research and Applications 07(04):27-36.
9) AZOM materials for stainless steel Grade 630.
10) Duplex and Super duplex by Cadence Engineering Services Ltd U.K.
11) 630/17-4PH Martensitic precipitation hardened stainless steel: AZO materials.
12) Metals Handbook -17-4 stainless steel 9th Ed. Vol.4, ASM.
13) Ambica steels, Grade 17-4PH Stainless steel manufactured at Ghaziabad location.

PREDICTION MODEL FOR THE BALLAST MARINE WATER QUALITY

Komathy K.

Abstract

Ballast water tank carries water from various seas and oceans and this, in fact, may lead to bio-invasion. Monitoring ballast water quality has thus become more vital so as to plan and implement an optimal treatment process before it exits to sea/ocean. The aim of this study is to assess the physiochemical characteristics of ballast marine water and to determine whether the water complies with standard norms stipulated by International Maritime Organization (IMO) so that the marine ecosystems are alive and healthy. A *prediction model is proposed in this paper using the machine learning technique called regression for the dataset covering the physiochemical values of eighteen seas and oceans. The paper also presented the outcome of the validated model for its goodness-of-fit against the Atlantic Ocean ecosystems and found to fit the dataset.*

Key Words: Physiochemical properties of marine water, regression analysis, goodness-of-fit of the model, multivariate regression, residual analysis.

INTRODUCTION

Ballast water tank in a ship is a fundamental aspect for maintaining the stability of the ship while loading and unloading goods, oil or passengers. Water extracted from one ocean or sea is flushed into another, which impacts the environment of the recipient ocean or sea by letting in harmful organisms such as bacteria and virus. To control and manage the water exchange activity of the ballasting and de-ballasting, International Maritime Organization (IMO, 2017) has devised a set of guidelines. Water quality indicators namely temperature, pH, total dissolved solids (TSS), dissolved oxygen (DO) and total suspended solids (TSS), are the prime components to regulate the quality of freshwater or marine water. The aquatic temperature controls certain toxins with the help of atmospheric oxygen. The pH alters the water to acidic, neutral, or alkaline based on the amount of hydrogen ions present in water. Living organisms survive on the dissolved oxygen in water. Turbidity indicates the suspended particles in water such as plankton, microbes or sediments. Specific conductance associated with electrical conductivity fluctuates as to cope up with water temperature and salinity. Salinity has resulted from the dissolved salts present in the water in the form of calcium, sodium, potassium, magnesium, chloride, sulphate. Water bodies such as rivers and streams carry more silts and sediments than calm water.

Water quality keeps falling as a result of industry automation, dumping of oil and other urban development activities. As a result, the ocean and river ecosystems become unsafe for aquatic living organisms due to various polluting resources. In the recent time, human health is continually challenged by the waterborne infections, contaminated seafood, and chemical toxins. Towards monitoring the quality of the treated of ocean/sea water from the ballast water tank, this paper has attempted to build a generic quality reference model where physiochemical factors are considered from various kinds of waterbodies whereas an inference model analyses the ocean data based on the spatial and temporal features of the new recipient ocean/sea to infer the suitability of the ballast water to let the water into a new water region. Regression is one of the machine learning techniques applied to predict the physiochemical properties, which is derived from the history of data, before the ballast water is let out based on the recipient water region. This paper has explained the reference model developed based on the dataset and as well the validating the model using Atlantic Ocean. Similar to the regression analysis followed for the Atlantic Ocean, other sea/ocean could also be validated.

REVIEW OF RESEARCH WORKS ON WATER QUALITY MONITORING

Marine water quality monitoring and management system (Yang 2019) was modelled on data mining technique, which was developed with the aim of preserving marine life and resources. It was a web-based remote system designed to monitor specifically rivers, lakes, and coastal sea. It monitored the parameters such as water temperature, dissolved oxygen and pH in the chosen time interval. Madeswaran et al. (2018), in their technical report, laid down the methods to observe the water quality parameters under spatial or temporal changes. They introduced the concept on water quality index (WQI) to reduce the complexity of the dataset so that it can be assessable by the policy makers. The aim of WQI was to examine the impact of sewage and domestic discharges on the coastal water quality. The study further recommended the use of WQI maps by the decision makers for realising immediate changes in the existing legislations to protect the coastal water quality of India.

The research study (Demetillo et al. 2019) developed a low-cost water quality monitoring system that was attributed for its long-term operation, adaptability, and reproducibility. Wireless sensor network was employed to precisely monitor water quality parameters and distributed the real-time results on the web, providing sufficient information on the current state of water quality in the covered areas. Chennai, one of the industrial hubs in India, spans to a larger coastal belt of Bay of Bengal, but poses often challenges caused by untreated sewage brought in by the Adyar and Cooum rivers. Prediction-based water quality model (Mishra et al. 2015) helped to find the movement of pollutants. High piling of biological oxygen demand, total suspended matter, PO4, and SiO4 during both wet and dry seasons were due to the influence of sewages on coastal waters, but reduction in salinity and dissolved oxygen were indicated at mixing zones. In addition to sewage, rise in air and water temperatures and reduction in pH were identified due to the influence of the physical elements. High stacking of nitrogen components in both seasons indicated the input from land inflow.

Kumar et al. (2020) proposed a real-time prediction model based on the dynamics of water quality. It was designed on a web-based service with built-in query processing to respond to queries promptly. The coastal authorities and stakeholders were alerted by the system instantly to mitigate the time lag or human errors.

High piling of biological oxygen demand, total suspended matter, PO4, and SiO4 during both wet and dry seasons were due to the influence of sewages on coastal waters, but reduction in salinity and dissolved oxygen were indicated at mixing zones

The prediction water quality model for Chennai coastal waters developed by Panda et al. (2020) was to determine the flow pattern of pollutants using dynamics of water and deterministic hydrology from the hydrological data captured from the coast. The model predicted the parameters such as temperature, salinity, dissolved oxygen, biological oxygen and coliform.

The coastal storm water drainage in Taylor's Creek, North Carolina (Fisher 2019) became a matter of concern when it was identified the increasing concentrations of faecal indicator bacteria in recreational waters following the inflow from heavy rainfall mixed with polluting sewage and wastes of the land, which are the reason for gastrointestinal diseases and other illnesses. In storm and ambient circumstances, this research study discovered patterns of pollutants and pathogen piling. The study also identified that the impact of high percentage of faecal indicator bacteria, which inhabited into the storm water drainage system of Taylor's Creek, even during dry weather. Salvi et al. (2014) have analysed the physiochemical properties of sea water, which are very critical for the health of the biodiversity in the Gulf of Kutch, Gujarat State, India. The results highlighted the changes in season and locality influenced the most of water quality parameters. The temperature and pH from the sampled sites were found to be complementing the marine biodiversity whereas the dissolved oxygen, total hardness, conductivity, turbidity, phosphate and nitrite showed a maximum in the samples from Okha and minimum in the samples of Sikka.

Pondicherry mangrove situated on the southeast coast of India provides the best breeding places for the most of marine fishes and shell fish. The study on these mangroves (Satheeshkumar and Khan 2009) showed a strong correlation between physiochemical and sludge residues. Salinity showed variation by the landscape, characteristics of the tide and inflow of the freshwater. The study inferred that pH had a significant role in determining the mangrove water quality. Further, the pH value was influenced by the concentrations of salinity and dissolved oxygen whereas the salinity and temperature were inclined towards one another. Dissolved oxygen was found to be low during summer and was biased by the sulphide concentration as well. Raju et al (2017) studied the impact of meteorological and physiochemical parameters of Arasalar estuary, Bay of Bengal, India. Water temperature rises gradually from monsoon to summer as a result of atmospheric conduction and radiation. The values of pH had touched the maximum during summer and reduction in pH during monsoon was seen due to the entry of fresh water from river and rainfall and the decay of biological matter. The amount of dissolved oxygen got altered by photosynthetic activity, floods, and wind turbulence. Dissolved oxygen was lower during the summer compared to monsoon. The visible change in the salinity was observed due to the high-raised tide in

the Arasalar estuary. The study concluded that though the seasonal changes in physiochemical parameters have not influenced the biological diversity of Arasalar estuary, it is predicted that the percentage of heavy metals in water would gradually increase.

The presence of physiochemical components, decomposition of aquatic life and the incidence of organic toxins cause the discrepancy in the pollution elements accumulated in sea water. Physiochemical pollution dynamics depend on temperature, conductivity and total suspended solids whereas pH and DO are related to chemical oils and fats affect the organic pollutants. The study by Hamzah et al. (2016), over the sea-passage between Johor Bahru and Singapore, found that more pollutants were generated due to organic disturbance created to the DO levels of aquatic life. High values of total suspended solids and pH were recorded for the western and eastern parts of the Johor Strait, which pointed towards chemical pollution.

Bhadja and Kundu (2012) studied the open sea coastline of Arabian Sea, India and found that temperature influenced the physiochemical properties of coastal water. High pH levels were found in two places namely Veraval and Diu due to high human intervention in these two localities. The inflow of freshwater and decomposition of organic matter have made the pH to reach low during monsoon. The rough tidal activity has raised the solid levels, thereby varying the conductivity. Due to the rough sea condition of the Arabian Sea and the monsoon wind, the conductivity was substantially higher during the monsoon season. Variation in total dissolved solids and salinity has made the electric conductivity to oscillate accordingly. However, it was noted that not much variation in total dissolved solids and suspended soil particles in these seawaters. Pitchaikani et al. (2016) evaluated the seawater quality in Digha, on the Bay of Bengal, north-western shore of India. The dissolved oxygen for biological organisms to break down organic material present in the water, dissolved solids, and nourishments for the growth of lives in the region were found to be within the permissible limits. Despite the fact that sewage was discharged into coastal seas, the water quality was unaffected. It could be because of the enormous amount of estuary water entering the system from the Hooghly estuarine system. The authors have observed that the presence of coastal tide and the undercurrent in coastal area have reduced the sewage effect on coastline water.

REGRESSION MODEL FOR PREDICTING THE BALLAST MARINE WATER QUALITY

Statistical properties of the dataset considered for the study

This paper has studied and analysed the dataset extracted from the Ocean Archive System (OAS) with accession no.0171017 (Boyer et al., 2018; NCEI, 2018a; NCEI, 2018b), which is an open public database maintained by National Centres for Environmental Information (NCEI) for historical data on Earth such as atmospheric, coastal, oceanic, and geophysical data collected from institutions, government agencies and individual researchers. Different ecosystems namely coastal, coastal upwelling, coral reef, deep hydrothermal vent, estuary, glacier, mangrove, mudflats, open ocean/sea, open ocean upwelling are covered in the dataset. The dataset was utilised for training and validation of the regression model developed for ballast water. The dataset is an open public database hosted by NCEI, who supported the research groups to investigate (Boyer et al. 2018). Arabian Sea, Arctic Ocean, Atlantic Ocean, Baltic Sea, China Sea, IAPSO, Indian Ocean, Mediterranean, Pacific Ocean, Red Sea and Southern Sea were some of the seas and oceans, for which the data were extracted from the NCEI dataset. The data pre-processing process, as a first step, was applied on the dataset to remove the missing values and outliers. Descriptive statistical measures were applied on the quality parameters from the dataset for all the ecosystems namely coastal, coastal upwelling, coral reef, deep hydrothermal vent, estuary, glacier, mangrove, mudflats, open ocean/sea and open ocean upwelling. The statistic descriptions presented in **Figure 1** represents the minimum, maximum, mean and standard deviation for marine water quality parameters namely total alkalinity (TA), dissolved inorganic carbon (DIC), salinity, temperature, dissolved oxygen (DO), pH and CO_2 for each of the ecosystems. Referring the optimum values listed in (Bhuyan et al., 2020; Stephanie, 2008; Twomey et al., 2009), the quality parameters mined from the dataset were found to be residing within the optimum range.

Attributes	MIN	MAX	Mean	Std. Dev	Attributes	MIN	MAX	Mean	Std. Dev
Coastal Sea					Coastal Upwelling				
Temp °C	-1.79	31.5	11.609	8.950	Temp °C	2.689	16.78	10.901	3.821
Salinity	0.0	40.4	32.399	6.684	Salinity	32.514	35.105	33.781	0.878
TA µmol/kg	1877.84	2618.4	2304.563	97.448	TA µmol/kg	2166.8	2436.2	2255.443	56.762
DIC µmol/kg	1783.15	2384.8	2103.190	86.948	DIC µmol/kg	1942.9	2338.0	2149.603	107.479
DO µmol/kg	15.6	467.68	264.480	65.152	DO µmol/kg	0.068	311.7	159.2	117.635
pH	7.28	8.792	8.066	0.188	pH	7.521	8.188	7.831	0.198
CO_2 µmol/kg	104.282	2912	423.589	329.426	CO_2 µmol/kg	252.569	1496.9325	750.102	361.641
Coral Reef					Deep Hydrothermal Vent				
Temp °C	27.7	29.3	28.140	0.658	Temp °C	-0.1061	30.285	7.786	10.146
Salinity	35.031	37.92	37.250	1.242	Salinity	34.596	36.837	35.065	0.736
TA µmol/kg	2273.6	2297.0	2287.259	10.175	TA µmol/kg	2274.0	2476.25	2391.451	65.491
DIC µmol/kg	1929.0	1958.4	1945.22	13.260	DIC µmol/kg	1929.0	2387.72	2256.86	138.986
DO µmol/kg	194.53	212.46	200.882	7.807	DO µmol/kg	12.4	346.7	140.79	95.783
pH	8.011	8.0	8.031	0.012	pH	7.732	8.119	7.861	0.143
CO_2 µmol/kg	376.983	409.537	387.968	13.244	CO_2 µmol/kg	309.178	894.891	553.776	159.705
Estuary					Glacier				
Temp °C	12.1	21.4	16.865	4.156	Temp °C	3.421	3.881	3.722	0.261
Salinity	2.8	35.3	23.498	13.299	Salinity	32.978	33.641	33.321	0.332
TA µmol/kg	2194.1	2343.3	2271.093	72.55	TA µmol/kg	2184.5	2227.5	2206.5	21.517
DIC µmol/kg	1987.2	2180.8	2092.863	94.112	DIC µmol/kg	1998.8	2041.0	2017.866	21.391
DO µmol/kg	191.4	293.6	236.081	39.744	DO µmol/kg	337.72	367.612	350.816	15.285
pH	7.812	8.641	8.12	0.349	pH	8.177	8.193	8.184	0.008
CO_2 µmol/kg	133.141	737.738	471.126	283.811	CO_2 µmol/kg	252.555	264.894	258.472	6.185
Mangrove					MudFlats				
Temp °C	25.6	28.2	26.9	1.838	Temp °C	27.11	30.01	28.56	2.05
Salinity	36.9	37.3	37.099	0.282	Salinity	36.55	36.79	36.67	0.169
TA µmol/kg	2289.1	2295.2	2292.149	4.313	TA µmol/kg	2268.2	2298.5	2283.35	21.425
DIC µmol/kg	2170.4	2190.7	2180.55	14.354	DIC µmol/kg	2150.5	2161.8	2156.15	7.99
DO µmol/kg	166.67	174.3	170.485	5.395	DO µmol/kg	182.31	201.72	192.015	13.724
pH	7.588	7.594	7.591	0.004	pH	7.573	7.654	7.613	0.057
CO_2 µmol/kg	1272.24	1286.71	1279.475	10.231	CO_2 µmol/kg	1094.611	1337.789	1216.2	171.952
Open Ocean Sea					Open Ocean Upwelling				
Temp °C	-1.926	30.06	8.39	9.286	Temp °C	1.869	2.142	1.973	0.117
Salinity	9.7	37.3317	34.543	2.0218	Salinity	34.647	34.664	34.657	0.007
TA µmol/kg	1906.3	2441.2	2312.599	57.625	TA µmol/kg	2412.4	2420.4	2415.9	4.123
DIC µmol/kg	1778.6	2388.2	2134.824	86.19	DIC µmol/kg	2336.7	2344.7	2339.95	3.403
DO µmol/kg	11.6	454.1	243.307	70.753	DO µmol/kg	94.0	110.0	103.0	6.683
pH	7.315	24.041	8.05	0.727	pH	7.76	7.803	7.7845	0.021
CO_2 µmol/kg	7.934	1850.282	418.124	206.448	CO_2 µmol/kg	571.223	636.317	599.305	32.674

Figure 1. Descriptive statistics of physiochemical properties for various ecosystems of oceans and seas extracted from NCEI dataset

Figure 2 displays the scatter diagrams representing the characteristics of physiochemical for the ecosystems of Atlantic Ocean. For each of the quality characteristics such as DIC, DO, pH, CO2, TA and salinity, the relationship against the temperature of the water, depth of the sea and distance from the nearest land area were examined. It is

ANGLO EASTERN
MARITIME TRAINING CENTRE

AEMTC MUMBAI : 401, Fourth Floor, Leela Business Park, Marol, Andheri-Kurla Road, Andheri (East), Mumbai-400 059.
T. +91 22 6720 5600 / 611 / 618 | A.O.H. +91 9820917656
aetr.bom@angloeastern.com
Capt. K. N. Deboo, Mr. Francis Akkara, Mr. Ivor Wilson

AEMTC DELHI : A-101, Dayanand Colony, Lajpat Nagar- 4, New Delhi - 110 024
T. +91 11 2642 6801 / 802 / 2647 2831 / 2647 1129
aetr.del@angloeastern.com
Capt. Prashant Gour, Ms. Sukhjeet Kaur

www.maritimetraining.in

MAN | PrimeServ



ME-C Control System Standard Operation (OEM Approved Course) **MAR'23 : 27 - 31**

For bookings: PrimeServ.academy-cph@man-es.com | aetrbom@angloeastern.com

WÄRTSILÄ

Wartsila RT Flex Engine **March 2023 : 13 - 17**

Conducted by Wartsila Switzerland (OEM Approved Course)


HYDRAULICS TRAINER


INSTRUMENTATION LAB


MAIN SWITCH BOARD


ENGINE ROOM SIMULATOR


HIGH VOLTAGE LAB

D. G. Approved Courses

		April 2023
1.	Refresher and Updating Training Course for all Engineers (RUTC)	03 - 05

Value Added Courses

		March 2023
1.	Advanced Marine Electrical course Module 1 - Practical Marine Electrical (Basic)	06-11, 20-25, 27-31
2.	Advanced Marine Electrical course Module 2 - Practical Marine Electrical (Advanced)	13-15, 27-29
3.	Advanced Marine Electrical course Module 4 - Electronics for Marine Engineers	02-03,16-17, 30-31
4.	Advanced Marine Electrical Course Module 5 & 6, Instrumentation, Process Control & Programmable Logic Controllers	06-11, 20-25
5.	Bridge Manouervering & Engine Control - Operational Level	02-03, 16-17
6.	Bridge Manouervering & Engine Control - Management Level	08-10
7.	Engine Room Emergency Management	16-17, 30-31
8.	Hydraulics for Engineers - Basic	13-15
9.	Hydraulics for Engineers - Advance	27-31
10.	Machinery Breakdown Safety Campaign - 2	17,13
11.	Maritime Crew Resource Management (MCRM)	06-10, 20-24
12.	Maritime Safety Management - Module 1 (Occupational and Behaviour Based Safety)	13-15, 27-29
13.	Maritime Safety Management - Module 2 (Risk Assessment)	06,20
14.	Maritime Safety Management - Module 3 (Shipboard Safety Officers)	08-21
15.	Maritime Safety Management - Module 4 (Accident Investigation-2)	09-23
16.	Port State Control (Online)	20-21
17.	SIRE 2.0 Training for Crew (Online)	13-27

1st in India and 2nd in the world to receive distinction by DNV SeaSkill Benchmarking

observed from **Figure 2** that the data were able to settle around the mean values of the parameters.

To validate the regression model for predicting the water quality of ballast water, the Atlantic Ocean water data samples from the dataset were extracted and tested the fitness of the model. This section focused on the design and validation of the regression model for the goodness-of-fit. R-square statistic helps to measure the goodness-of-fit for a linear regression model (Montgomery et al. 2012) and it represents the data variability against its mean. It is represented on a scale of 0 to 1 or in percentage 0 to 100. While correlating the relationship between an independent and dependent variable, R-square denotes the amount of variance the independent variable is associated with the dependent variable. This study has applied Microsoft Analysis Toolpak and Anaconda with Python and Pycaret programming tools for creating and assessing the prediction using the regression model.

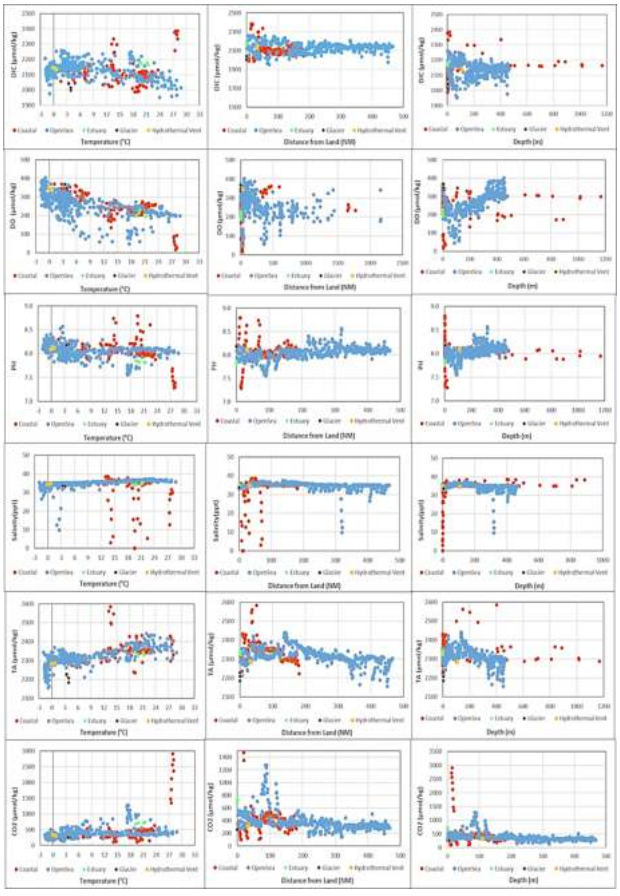

Figure 2. Scatter diagrams representing physiochemical properties for various ecosystems of Atlantic Ocean

Linear regression analysis of Atlantic Ocean water

Visual graphs play a significant role to interpret the outcome of the regression analysis rightly than the calculated numbers alone. First, the linear regression models were generated for the observations of six independent indicators namely DIC, DO, pH, CO2, TA and salinity. Those observed values were mapped against their predicted values and the consolidated outcomes are presented in **Figure 3**. Presence of negative slopes of the graphs suggested that the dependent variable tends to decrease as the independent variable increases. Negative slopes of the linear regression lines for some of the parameters were highlighted in the **Table 1**. DIC has correlated negatively with temperature, distance and depth; DO with distance and depth; pH with temperature, distance and depth; TA with depth; salinity with distance and depth and CO_2 with distance and depth.

Further, the results of analysis of variance (ANOVA) were significant in the regression analysis with values of f-statistic and p-value. The p-value of each dependent parameter validated the null hypothesis, which stated that the parameter is not correlated with the independent. Most of the estimated p-values were less than the significance level (usually 0.05) and hence, the prediction model for the water quality parameters fitted the data well. Table 1 displays the p-values as well.

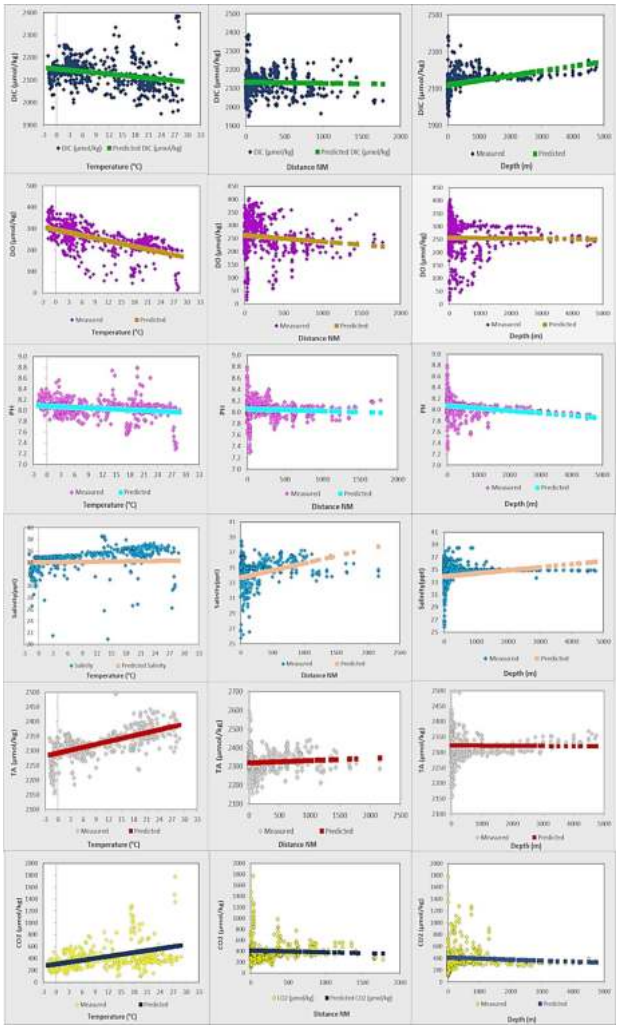

Figure 3. Linear regression analysis of physiochemical properties of Atlantic Ocean

Table 1 also included the R-squared and standard error for each of the regression line analysed. It is principally true if the dependent variable does not respond to the variation of the independent variable, it will yield lower R-squared value. Though the independent variables were

correlated well with the dependent variables, it is observed from the Table 1 that the variability of certain dependent variables around the mean were very high. However, it is observed that the residuals were randomly spread around the zero-regression line, which inferred that the model fitted the dataset. **Table 2** lists the prediction equations for the quality parameters considered for Atlantic Ocean. The estimated values of regression coefficients say, the y-intercept and the coefficient of the quality parameter have helped to arrive at the prediction equations as given in **Table 2**.

Table 1. Linear Regression analysis of physiochemical properties of Atlantic Ocean

Parameter		R-Squared	Standard Error	p-value
DIC (µmol/kg)	Temp(°C)	0.1893	46.17	0.0
	Distance(NM)	0.0012	58.75	0.37
	Depth (m)	0.5099	43.35	0.0
DO (µmol/kg)	Temp(°C)	0.1640	53.75	0.0
	Distance(NM)	0.0172	63.62	0.0007
	Depth (m)	0.0003	64.16	0.65
TA (µmol/kg)	Temp(°C)	0.4144	35.19	0.0
	Distance(NM)	0.0084	45.8	0.018
	Depth (m)	0.0001	45.99	0.76
Salinity (ppt)	Temp(°C)	0.0004	4.348	0.613
	Distance(NM)	0.0222	4.30	0.0001
	Depth (m)	0.0114	4.323	0.0059
pH	Temp(°C)	0.0485	0.1541	0.0
	Distance(NM)	0.0059	0.1576	0.048
	Depth (m)	0.0721	0.1522	0.0
CO_2 (µmol/kg)	Temp(°C)	0.1490	231.64	0.0
	Distance(NM)	0.0018	250.87	0.276
	Depth (m)	0.0042	250.57	0.096

Table 2. Linear regression equations representing the prediction of physiochemical parameters

Dependent variable	Independent variable	Linear regression equation
DIC (µmol/kg)	Temp(°C)	-1.919 x Temp +2149.6
	Distance(NM)	-0.006 x Dist + 2133.72
	Depth (m)	0.025x Dep + 2118.6
DO (µmol/kg)	Temp(°C)	-4.35x Temp + 295.42
	Distance(NM)	-0.0245 x Dist + 262.11
	Depth (m)	-0.0012 x Dep + 256.62
TA (µmol/kg)	Temp(°C)	3.310 x Temp + 2292.4
	Distance(NM)	0.0123 x Dist + 2319.07
	Depth (m)	-0.0006 x Dep + 2322.44
Salinity (ppt)	Temp(°C)	0.0095 x Temp + 34.06
	Distance(NM)	0.0019 x Dist + 33.68
	Depth (m)	0.0005 x Dep + 33.89
pH	Temp(°C)	-0.0039 x Temp + 8.08
	Distance(NM)	-3.53E-05 x Dist + 8.05
	Depth (m)	-4.54E-05 x Dep + 8.07
CO_2 (µmol/kg)	Temp(°C)	10.84 x Temp + 304.99
	Distance(NM)	-0.031x Dist + 410.96
	Depth (m)	-0.0174x Dep + 412.49

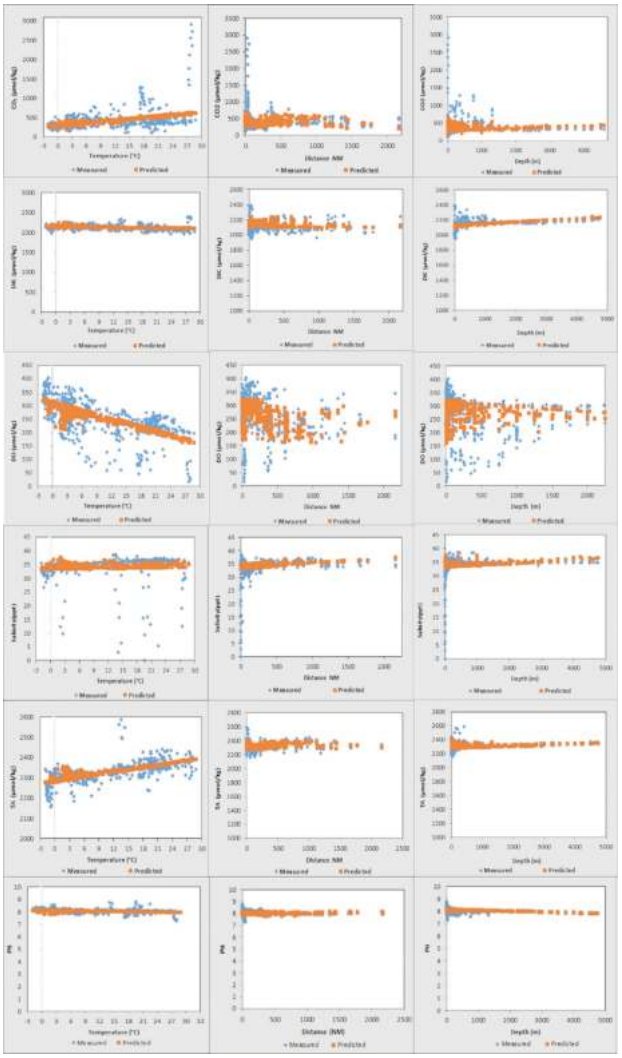

Figure 4. Multivariate regression lines-of-fit for Atlantic Ocean

Multivariate linear regression (MVLR) analysis for the ballast water

Multiple regression statistics helps to predict the dependent variable if it depends on more than one independent variable. In the investigation, the temperature, distance and depth were considered as the contributors whereas DIC, DO, TA, salinity and CO_2 were taken as the dependent parameters individually. The multivariate equation with three independent variables to suit our model is given in Equation (1).

$$y_i = b_0 + b_1 x_{i1} + b_2 x_{i2} + b_3 x_{i3} + e \quad (1)$$

where, i varies from 1 to n observations; y_i is the expected or predicted outcome; x_{i1}, x_{i2} and x_{i3} are the observed variables; b_0 represents the y-intercept; b_1, b_2 and b_3 are the slope coefficients for each of the independent variables; and e is the residual. **Table 3** lists the expected outcomes of salinity, total alkalinity, DIC, DO, pH and CO_2 using the multiple linear regression coefficients as given in Equation (1). The plotted graphs portrayed in **Figure 4** for the complete Atlantic Ocean ecosystems illustrating the characteristics of observed verses the predicted data.

Table 3 shows the regression coefficients for salinity, total alkalinity, DIC, DO and CO_2 when multiple parameters namely temperature, distance and depth were correlated. The multivariate regression equations given in **Table 3** represented the independent variables namely temperature (Temp), distance (Dist) and depth (Dep). **Table 4** lists the regression statistics under multivariate analysis. Standard error is the average distance of the observed values away from the regression line. Multiple R represents the square root of the R-square. Adjusted R-squared is used if more than one dependent variable. Referring to **Table 1** and **Table 4**, the R-squared values were found to be below 50% for both linear and multi variate regression models. In such cases, the residual graphs would help us to assess whether the points are randomly spread around zero residual line. If so, it is unbiased and this residual pattern indicates a good fit despite the low R-squared.

Residual helps to measure the how far the estimated predicted value of the parameter is nearer to its corresponding observed value and is represented as a vertical distance between the observed data point and the line-of-best fit. The estimated residual is positive if the point is above the regression line; negative if it is below the regression line; and zero if the point lies on the regression line. To illustrate the linear regression model is unbiased, residuals were mapped for the quality parameters and then the ensuing eighteen scatter plots were consolidated in **Figure 5**. From **Figure 5**, the residuals are found to be scattered randomly around the zero residual line. This concluded that a multivariate linear model fits very well for modelling the marine water quality dataset.

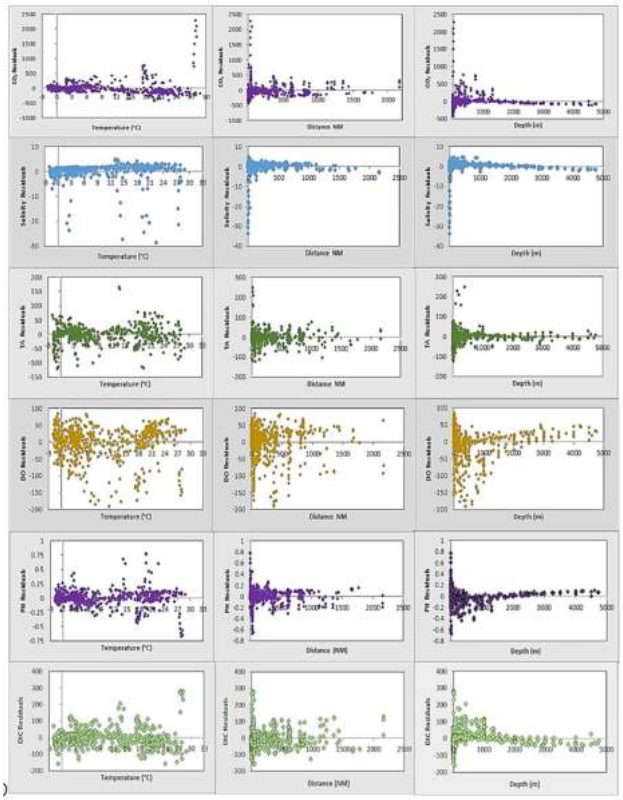

Figure 5. Multivariate residual plots for physiochemical indicators to illustrate the model is unbiased

Table 3. Coefficients of multiple regression equation for water quality parameters of Atlantic Ocean

Coefficients	Salinity (ppt)	TA (µmol/kg)	DIC (µmol/kg)	DO (µmol/kg)	CO_2 (µmol/kg)	pH
y-intercept (b0)	33.209	2280.027	2132.538	314.809	293.404	8.143
Temperature coefficient(b1)	0.0267	3.799	-1.0338	-5.052	12.003	-0.00653
Distance coefficient (b2)	0.0017	0.0034	-0.0114	-0.012	-0.055	-6.23E-06
Depth coefficient (b3)	0.0005	0.0128	0.0223	-0.018	0.0275	-6.83E-05

Table 4. Regression statistics for Atlantic Ocean

Regression Statistics	Salinity (ppt)	TA (µmol/kg)	DIC (µmol/kg)	DO (µmol/kg)	CO_2 (µmol/kg)	pH
Multiple R	0.1816	0.689	0.438	0.664	0.4019	0.1816
R Squared	0.0330	0.475	0.192	0.440	0.161	0.033
Adjusted R-squared	0.0286	0.472	0.188	0.438	0.158	0.0286
Standard Error	4.283	33.375	52.937	48.071	230.27	4.283

A World-Class
VIRTUAL REALITY LAB

D. G. SHIPPING APPROVED

MEO Class 2
Preparatory Course

1st of Every Month

Vizag & Chennai

MEO Class 1
Engineering Management

1st of Every Month

Chennai

REO
Revalidation course for all Engineers and ETO's

Every Week

Vizag & Chennai

Basic IGF
Basic Training for Ships using Fuels covered within IGF code

DURATION 4 DAYS

EVERY MONTH

Advanced IGF
Advanced Training for Ships using Fuels covered within IGF code

DURATION 5 DAYS

EVERY MONTH

ERS
Engine Room Simulators\Operational Level
MEO CLASS - IV

Every Month - Multiple batches at Vizag & Chennai

ERSM
Engine Room Simulators
Management Level -MEO CLASS II

Every Month - Multiple batches at Vizag & Chennai

DECGS
Diesel Engine Combustion
Gas Simulator - MEO CLASS-I

Every Month - Multiple batches at Vizag & Chennai

HV
High Voltage Safety and Switch Gear – Management Level Course

Every Month

R-AFF
Refresher
Advanced Fire Fighting

Every Week

R-PSCRB
Refresher Proficiency in
Survival Craft Rescue Boats

Every Week

Hindustan Institute of Maritime Training
Online Booking at www.himt.co.in

www.himtmarine.com | www.himtcollege.com | www.himtoffshore.com | www.himtelearning.com

CONCLUSION

This paper has proposed a prediction model to analyse the physiochemical properties of the oceans and seas using the machine learning platform. This paper has analysed the dataset from NCEI and brought out the expected values based on linear and multivariate regression analyses. The model was built on the dataset covering eighteen number of seas and oceans. This paper has assessed the ecosystems of Atlantic Ocean with quality measures such as DIC, DO, pH, CO_2, TA against temperature, distance and depth. The outcome of the validation of the regression model using the data of Atlantic Ocean, indicated that the prediction model has shown an optimistic goodness-of-fit.

ACKNOWLEDGEMENT

Department of Science and Technology (DST), India sponsored the financial support for this research study under the scheme of optimal water usage for industrial sector (OWUIS).

REFERENCES

1. Bhadja, Poonam, and Rahul Kundu. (2012). "Status of the seawater quality at few industrially important coasts of Gujarat (India) off Arabian Sea". *Indian Journal of Geo-Marine Sciences,* Vol.41, No.3: pp.90-97.
2. Bhuyan, M. S., Mojumder, I. A., and Das, M. (2020). "The optimum range of ocean and freshwater quality parameters". *Annals of Marine Science*, Vol.4, No.1, pp. 19-20. https://dx.doi.org/10.17352/ ams.000020
3. Boyer, T. P., Baranova, O. K., Coleman, C., Garcia, H. E., Grodsky, A., Locarnini, R. A., ... and Zweng, M. M. (2018). "World Ocean Database 2018" *NOAA National Centers for Environmental Information. Dataset,* https://www.ncei.noaa.gov/access/metadata/landing-page/bin /iso?id=gov. noaa. nodc: NCEI-WOA18
4. Demetillo, Alexander T., Michelle V. Japitana, and Evelyn B. Taboada. (2019). "A system for monitoring water quality in a large aquatic area using wireless sensor network technology". *Sustainable Environment Research,* Vol. 29, No.1, pp. 1-9. https://doi.org/0.1186/s42834-019-0009-4
5. Fisher, Kinsey. (2019). "Characterizing Microbial Contaminants Flowing into Taylor's Creek, North Carolina." (https://doi.org/10.17615/7rqd-bx29.
6. Hamzah, F. M., Jaafar. O., Jani W. N. F. A., Abdullah, S. M. S. (2016). "Multivariate analysis of physical and chemical parameters of marine water quality in the Straits of Johor, Malaysia". *Journal of Environmental Science and Technology,* 9.6 (2016): 427-436. https://doi.org/10.3923/jest.2016.427.436.
7. International Maritime Organization (IMO). (2017). "2017 Guidelines for ballast water exchange (G6). Resolution MEPC.288(71)". https://wwwcdn.imo.org/localresources/en/KnowledgeCentre/IndexofIMOResolutions/MEPCDocume nts/MEPC.288(71).pdf
8. Kumar, Saka Sujith, Panda, U. S., Pradhan, U. K., Mishra, P., & Ramana Murthy, M. V. (2020). "Web-based decision support system for coastal water quality" *Journal of Coastal Research,* Vol.89, pp.139-144. https://doi.org/10.2112/SI89-023.1
9. Madeswaran, P. (2018). "Status report (1990–2015): Seawater quality at selected locations along Indian coast." *Nat. Centre Coastal Res., Chennai, India*.
10. Stephanie, Mc Caffery. (2008). "Water Quality parameters and Indicator". *Waterwatch New South Wales, Namoi Catchment Management Authority,* pp. 1-6.
11. Mishra, Pravakar, Panda, U. S., Pradha, U., Kumar, C. S., Naik, S., Begum, M., Ishwarya, J. (2015). "Coastal water quality monitoring and modelling off Chennai city". *Procedia Engineering,* Vol.116 (2015), pp.955-962.
12. Montgomery, Douglas C., Elizabeth A. Peck, and G. Geoffrey Vining. (2021). *Introduction to linear regression analysis,* John Wiley & Sons.
13. NCEI. (2018a). "Seawater Mg/Ca and Sr/Ca ratios worldwide from 2009 to 2017 collected in 79 cruises, including coupled measured data for temperature, salinity, total alkalinity, DIC, DO, and calculated pH and CO2: NCEI Accession 0171017". *National Centers for Environmental Information (NCEI),* (2018a). https://www.ncei.noaa.gov/access/metadata/landing-page/bin /iso? id=gov. noaa. nodc:0171017
14. NCEI. (2018b). "*OAS accession Detail for 0171017*". https://www.ncei.noaa.gov/archive/archive-management-system/ OAS/bin/prd/jquery/accession/details/171017
15. Panda, U. S., Pradhan, U. K., Kumar, S. S., Naik, S., Begum, M., Mishra, P., and Ramana Murthy. (2020). "Bathing Water Quality Forecast for Chennai Coastal Waters". *Journal of Coastal Research,* Vol.89(SI) pp. 111-117. https://doi.org/10.2112/ SI89-019.1
16. Pitchaikani, J. Selvin, K. Kadharsha, and Subrat Mukherjee. (2016). "Current status of seawater quality in Digha (India), north-western coast of the Bay of Bengal" *Environmental Monitoring and Assessment,* Vol.188, No.7, pp. 1-11. https://doi.org/10.1007/s10661-016-5383-3
17. Raju, C., Sridharan, G., Mariappan, P., and Chelladurai, G. (2017). "Physio-chemical parameters and Ichthyofauna diversity of Arasalar estuary in southeast coast of India". *Applied Water Science,* Vol.7, No.1, pp. 445-450.
18. Salvi, H., Patel, R., Thakur, B., Shah, K., Parmar, D. (2014). "Assessment of Coastal Water Quality Parameters of Selected Areas of Marine National Park & Sanctuary (Okha, Sikka & Khijadiya)". https://dx.doi.org/10.2139/ssrn.2456093.
19. Satheeshkumar, P., and B. Anisa Khan. (2009). "Seasonal variations in physio-chemical parameters of water and sediment characteristics of Pondicherry mangroves" *African Journal of Basic and Applied Sciences,* Vol.1, No.1-2, pp. 36-43.
20. Twomey, L. J., M. F. Piehler, and H. W. Paerl. (2009). "Priority parameters for monitoring of freshwater and marine systems and their measurement" *Institute of Marine Sciences, University of North Carolina at Chapel Hill, USA.*
21. Yang, G. (2019). "Marine Water Quality Monitoring and Management System Model Based on Data Mining" *Journal of Coastal Research,* Vol.94, pp. 11-15. https://doi.org/10.2112/SI94-003.1

About the Author

Komathy K currently serves as a Professor in the department of CSE, Academy of Maritime Education and Training, Chennai, India. She obtained her Doctor of Philosophy in Computer Science and Engineering from Anna University, India in 2008. Her research publications include wired, wireless networking, network security, internet-of-things, artificial intelligence, machine learning and so forth. She extends her expertise through professional societies such as CSI, ISTE, and IET in India.

Email: gomes1960@yahoo.com

LUBE MATTERS # 21

WEAR (PART II)

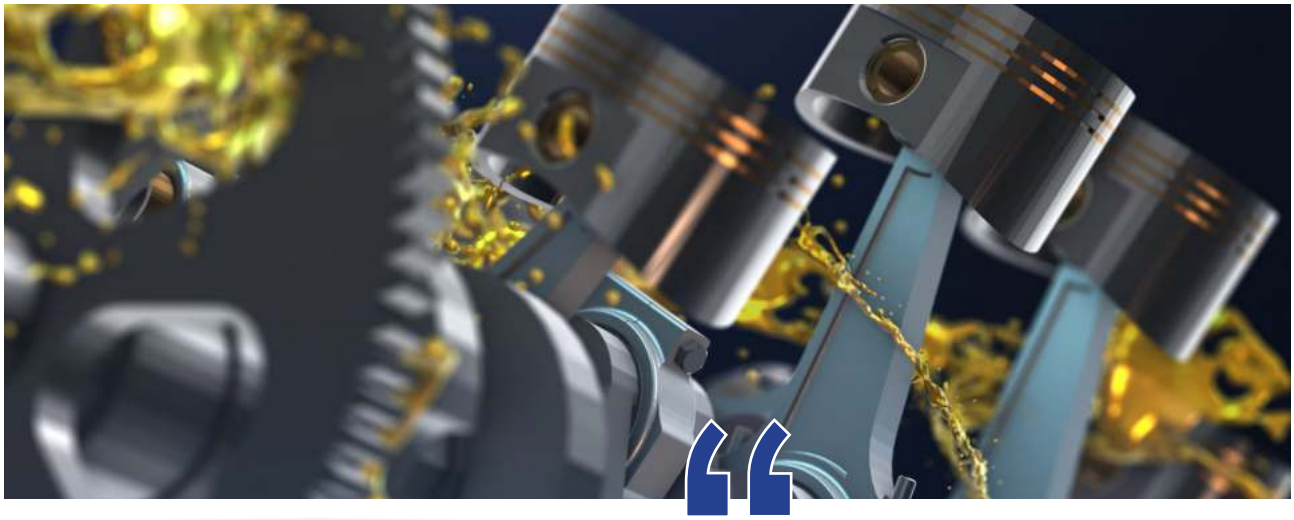

Sanjiv Wazir

> Fretting starts with adhesive wear due to microwelds between asperities

Fretting Wear

Fretting refers to small amplitude, high frequency, oscillatory motion (usually sliding) between two solid surfaces in contact. The limited distance of oscillation is typically smaller than the contact length, often less than 1 mm, so most wear particles remain within the contact region. Fretting starts with adhesive wear due to microwelds between asperities. Breaking of asperities causes pitting. The heat of the microwelding causes oxidation of fresh metal surfaces.

Fretting wear rate is affected by the kind of debris generated. Softer debris may deposit around asperities and carry some of the load and reduce wear rate. Harder debris may cause abrasion and increase wear rate.

Fretted surfaces are often rough, and in some materials this roughness may induce cracks which serve as sites for initiation of fatigue. In some cases, surface roughening may provide escape channels for debris. When fretting occurs in combination with corrosion, it is known as **fretting corrosion** (1).

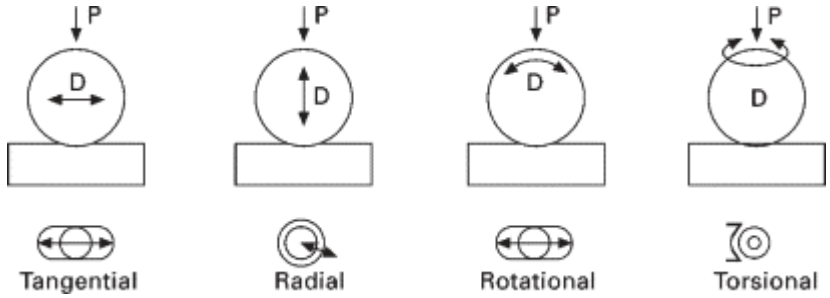

Figure. 1: Types of Fretting Wear (2)

Fretting loosens up some joints, seizes up others, and may provide a site for crack initiation. Fretting can occur between rivetted/bolted joints, at the back of bearing shells, gears on a shaft, splines, transformer cores, artificial hip joints and bone, etc.

Fretting wear can often be reduced by design changes to control the displacements and stresses in the contact. Reducing friction by means of a solid lubricant coating such as MoS2, or reducing asperity stresses by applying copper-based thick coatings can be beneficial in fretting wear contacts.

Pitting wear

Pitting is mainly observed in components in rolling and rolling/sliding contact. **The root cause of pitting is contact fatigue**. Cyclical stressing in a non-conformal rolling contact, over time leads to strain localisation or discontinuity at some defect in material eventually leading to crack initiation. The crack can be initiated at the surface or subsurface (3).

Crack initiation is followed by crack propagation, eventually resulting in the loss of a chunk of material leaving behind a crater or pit on the surface – this is **macropitting**. Although micropitting also occurs by a fatigue mechanism, it is caused by plastic fatigue of the asperities. The high stresses on the asperities of rough surfaces in rolling contact will exceed the yield stress and plastic deformation or "flattening" of the asperity will

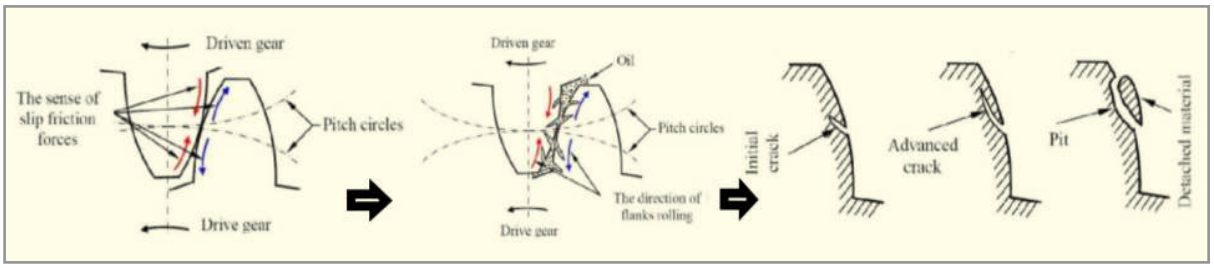

Figure. 2: Mechanism of initiation of pitting on gear flank (4)

occur. With repeated contact cycles, fatigue will occur, leading to eventual loss of the asperities in the form of micropitting (3).

Pitting is mainly observed in rolling element bearings, gears, and railway tracks.

Erosion

Abrasive erosion

When a moving fluid contains abrasive particles, wear will occur. If the velocity is low there may only be removal of surface films, but at high velocity, substrate material is worn away as well. In Abrasive erosion, concentrations of entrained particles are low, and the focus is on liquid flow. Where the liquid is acting as a carrier of solids, which is known as slurry, the resultant erosion is known as slurry erosion. Abrasive wear is used (abrasive Jet cutting) to cut through concrete and metals.

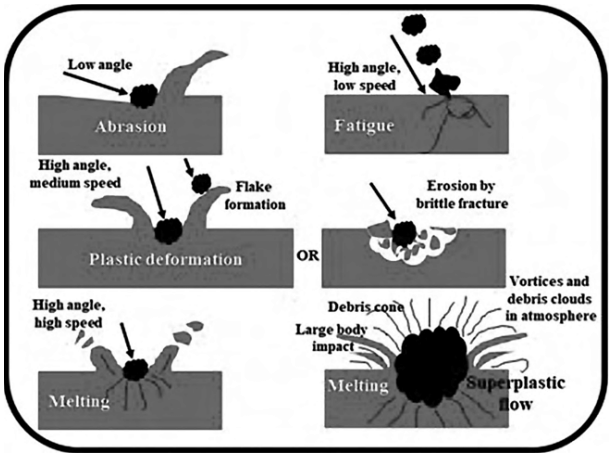

Figure. 3: Mechanisms of erosion by solid particle impact (5)

Erosion by (dry) solid particle impingement

Solid particles often have sufficient momentum to damage solid surfaces. Impingement of sharp and hard particles at low angles will abrade (cut) soft, ductile material. Material loss by cutting begins very soon after impingement begins. Particles of any shape and hardness, impinging at high angles, will fatigue surface material, causing loss, but the onset of loss is delayed as the material fatigues. Angular particles erode much faster than round particles. Hard and sharp particles may embed during impingement at high angles.

Particle size and particle velocity, impingement angle, relative hardness (compared to hit surface) are important parameters affecting erosion rates. Ductility is sometimes more important than hardness in resisting erosion.

Wear mechanisms, without solid-solid contact

Erosion by Liquid impingement

When liquid drops strike a solid surface with sufficient momentum and sufficient frequency, material may be removed from the surface by fatigue.

Cavitation

Cavitation refers to the formation and rapid collapse by implosion of bubbles that contain vapour or gas. When liquids flow through changing cross-sections, past obstacles (for example, a pipe), etc, the momentum of the different liquid streams may produce a local low-pressure zone than in the bulk liquid. If the pressure drops below the vapor pressure of the liquid, bubbles of vapor will form locally. When the liquid pressure rises, the bubbles collapse very quickly. The implosion of the bubble causes a spherical front of the liquid to rush into the cavity. Usually a cloud of bubbles is formed and some of them may implode on a solid surface.

There is sufficient momentum in the jet of liquid to strain the material in the impingement area. In most regions the strain is much less than the yield strain, but when elastic strains are imposed millions of times in small regions over a surface, local failure of material occurs by fatigue. This cavitation process, which commonly occurs when there is sudden drop in pressure of liquids, erodes away ship propellers, pipes, valves in pipes, and the vibrating cylinder walls of engines.

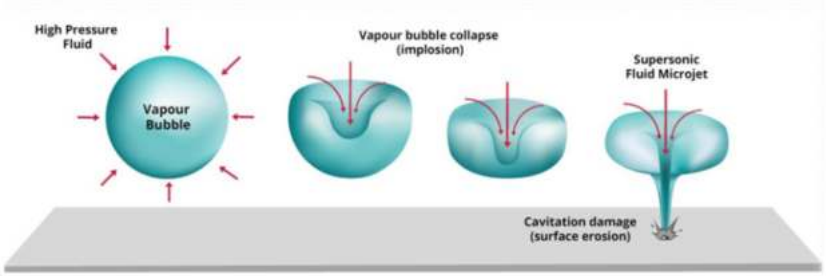

Figure. 4 : Mechanism of cavitation wear on pipe/pump vane surface (6)

Chemical wear

Oxidative wear

Chemical wear in air is generally called oxidative wear as oxygen is the dominant corrosive medium for metals in air. Oxides of metals often prevent seizure between rubbing surfaces. The rate of formation of oxide layer relative to the rate of mechanical destruction/removal of the oxide layer determines its protective strength.

The mechanism of oxidative wear is that the sliding surfaces heats up and oxidises at a rate that decreases with increasing oxide film thickness. At some point the film reaches a critical thickness and flakes off. Thus, the thicker the film becomes before it separates, the more slowly oxides form overall and slower will be the wear rate (2).

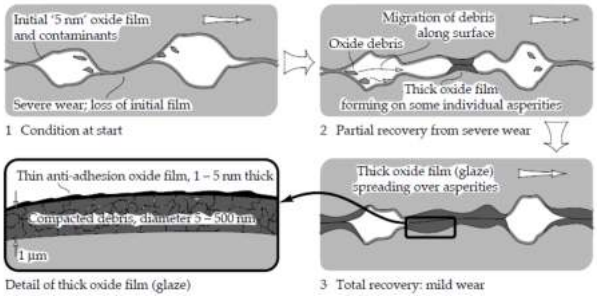

Figure. 5: Mechanism of oxidative wear at slow speed

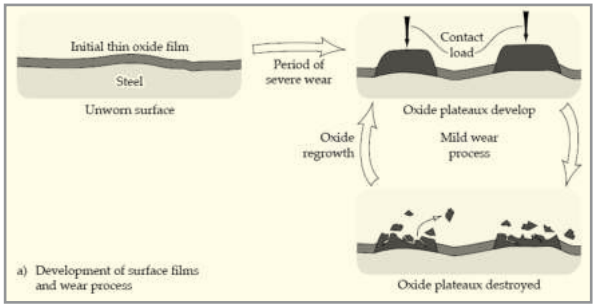

Figure. 6: Mechanism of sliding wear with changing speed (7)

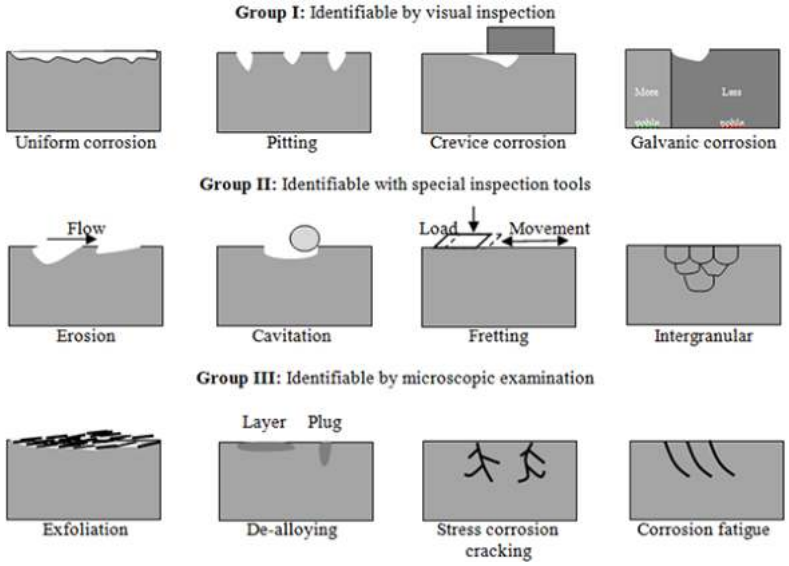

Figure. 7 : Main types of corrosion grouped by their ease of recognition(8)

Corrosive wear

Corrosive wear is damage caused to surfaces by chemical attack. Corrosive wear results when contact and relative motion between surface occurs in a corrosive atmosphere. Many materials form thin surface films that may slow or stop corrosion. However, if this layer is continuously destroyed or removed due to wear, corrosion of the base material will continue, and another corrosion layer begins to form. The process of repeated formation and removal of corrosive layer formation is corrosive wear. Major corrosive agents are atmospheric oxygen (oxidative wear), water and seawater, chemicals, acids, and other fluids.

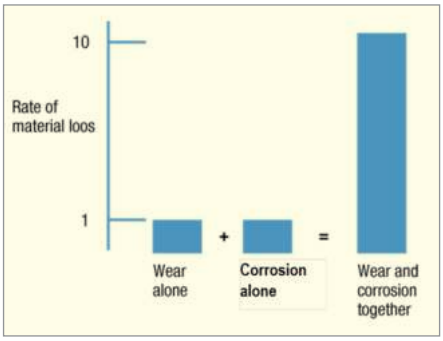

Figure. 8 : Comparison of rate of material loss by wear, corrosion and wear+corrosion (9)

Corrosion types can be classified according to the appearance of the corroded surface, viewed either by visual inspection or by a magnifying glass or microscope (**Figure. 5**). Since each form of corrosion has its characteristic causes, steps to

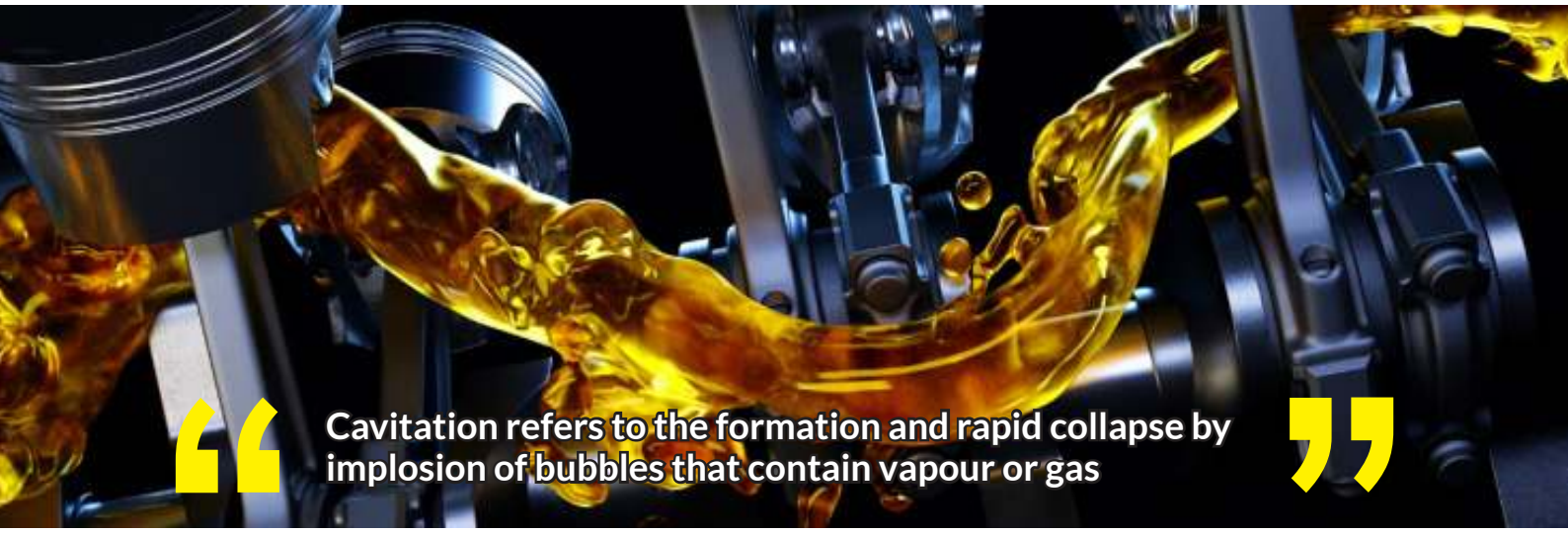

Figure. 9: Hot Corrosion of diesel engine valve (9)

prevent or minimise attack can often be suggested after identifying the underlying cause (7).

Factors Affecting wear

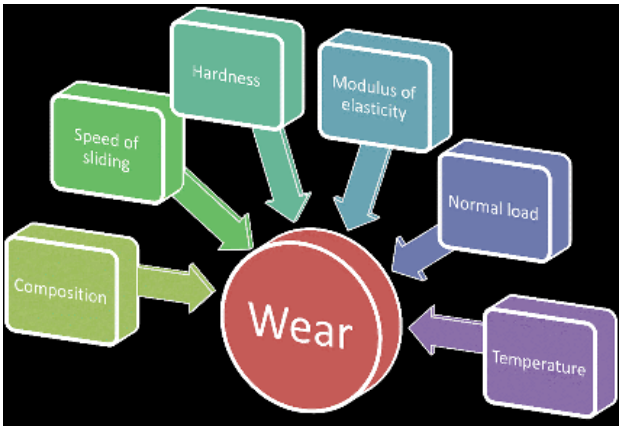

Figure. 10: Factors affecting wear.

Conclusion

The conditions to which a surface is exposed during wear are quite different from those involved in the measurement of conventional mechanical properties such as tensile strength, indentation hardness or fracture toughness. The dimensions of oxide or lubricant films, of surface height variation, or of wear debris, typically lie in the range from 10 nm to 1000 μm . In the absence of a thick lubricant film, surfaces make contact with each other at local asperities which interact and induce high stresses over distances of the order of micrometres on a timescale of the order of microseconds. Not only are the timescales very short and strain rates high, but all the energy of frictional work is dissipated through the interactions of these contacts, often leading to high but transient local temperatures. Even in a lubricated contact, the power density can be very high.

Significant efforts have improved our understanding of many aspects of wear mechanisms. Advances in materials, surface engineering and lubricants, as well as in design methods and condition monitoring, have led to major improvements in the efficiency, lifetime cost and performance of many engineering systems. However, challenges in tribology, especially in developing predictive wear rate models, remain.

References

1. G.W. Stachowiack, Editor, Wear-Materials, Mechanisms, Practice, 2006, pub: Wiley
2. P. Kapsa, Basics of fretting, ScienceDirect, 2011
3. Kenneth Ludema, O.O. Ajayi; Friction,Wear & lubrication, A text book of Tribology, 2nd Ed., CRC press
4. C.O Papa, S Haragas, The appearance of pitting wear on gears and some factors that influence it; 31/03/2018; Semantic Scholar
5. Erosive Wear, Researchgate
6. Valve Cavitation, SlurryFlo
7. Oxidative wear, Tribonet
8. Rana Afif Majed Anaee, Majid Hameed Abdulmajeed, Tribocorrosion, Advances in Triblogy, Ed. Pranav Darji,2016
9. Cold Corrosion in Marine 2-Stroke Engines, CIMAC Guideline 11/2117

About the Author

Sanjiv Wazir is an Adviser on marine lubrication. He is a mechanical engineer from IIT-Bombay. He is a marine engineer and a fellow of the Institute of Marine Engineers. He is a Certified Lubrication Specialist from the Society of Tribologists & Lubrication Engineers (STLE), USA and is a member of the Tribological Society of India. He has contributed to MER on marine lubrication developments in the past. He has written a series of articles on tribology & lubrication issue under 'Lube Matters'.

Email: sanjiv.wazir@gmail.com

TROUBLESHOOTING MARINE ELECTRICAL EQUIPMENT – PART 1A - THE FIRST CRUCIAL STEPS

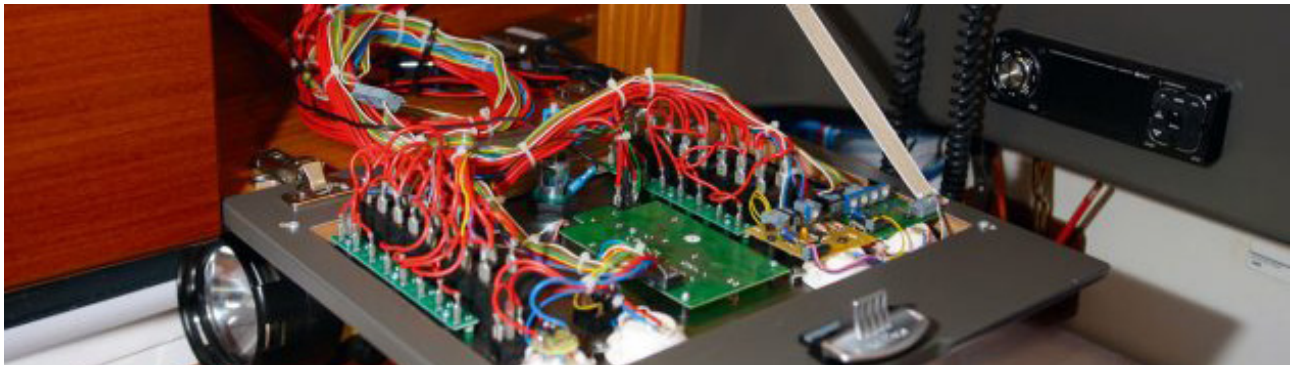

Elstan A. Fernandez

Abstract/Summary

This article is a first in a series of exclusive articles for MER that will attempt to highlight the various aspects of Maintenance and Troubleshooting of almost all commonly-used Electrical and Electronic Equipment onboard commercial ships. It is based on the current requirements of Marine Engineers and ETOs.

Key Points

- Factors to be considered while troubleshooting Marine Electrical equipment.
- An Alternative (logical) approach to troubleshooting

Introduction

Shipboard equipment can malfunction for a variety of reasons. Mechanical contacts and parts can wear out; wires can overheat and burn out; parts can be damaged by impact or abrasion; etc. Typically, whenever any equipment fails, there is a sense of urgency to get it fixed and working again. In the shipping industry, defective equipment could also cause unexpected loss of revenue and unprecedented loss of time.

It is thus essential to have a holistic understanding of the operation of equipment and general insight into some of the diagnostic skills used to solve any problem that occurs.

- Impulsive actions often lead to unforeseen and further complications; it is better to have a well-planned strategy. The evidence is carefully considered before deciding the action to be taken.
- Social skills are a must as no one can work in isolation. Often the fault can be solved because brighter minds and willing hands were there when you needed them the most.
- Persistence and physical fitness is a very good attribute as some issues take repeated and time-consuming attempts in order to achieve the desired results.

Factors to be Considered While Troubleshooting

1 System Knowledge

Understanding the basic operation of a system leads to eliminating most common faults. It is often said that presence of mind stems from knowledge gained. Troubleshooting is made easier when the main functional blocks can be identified and when correct operating procedures are followed.

Using a logical, systematic approach to analyse the circuit's behaviour is critical. Logical reasoning will reduce the time required to troubleshoot a fault. There are several approaches in use. They may have different steps or processes, but they have the following in common; they all approach problems systematically and logically thus minimising the steps and ruling out trial and error. In other words, it is a logical approach in understanding the behaviour of a system. As in the case of condition monitoring, this also involves collection of evidence, such as unusual sounds, vibration data, acrid smells, temperature variations, burn marks, etc.

Perception of the outcome of every action taken during the troubleshooting process will lead to positive results. Use of one's basic senses would also prove fruitful. An alternate approach is explained in article 8.6.6.

Possessing the right technical skills and experience are also essential - as although the problem itself may take a few minutes or even hours, it could result in damage to components and accidents if the right approach is not adopted.

The adequate use of instruments and analysis of the data that they display / log forms a basis of testing theories and assumptions, thus leading to precise fault identification and rectification.

2 System Configuration and Parameters

Locate all components, connections, and the origin of power supplies. Components as push buttons, contactors, various types of switches, relays, sensors, motors, etc., are the ones that generally malfunction.

We know that most electrical circuits control or operate mechanical systems and components; it is also important to understand the mechanical aspects of the equipment. You need to be able to determine how the circuit works under normal conditions and what effect can occur after changing the circuit inputs on the circuit operation. For example, what happens to the overall circuit operation when a push button is pressed, which relays energise, which lamps glow, does the pump start or stop, etc. You also need to be able to determine what effect a faulty component may have on the circuit operation.

Study the normal operating parameters or operating ranges of the system. More often, expectations don't match with reality.

3 Test Equipment

Learn to use basic test equipment properly. It helps in expediting fault-finding. The following approach is advisable:

- Most defects turn out to be simple. Think first! Start with the basics unless you know the history of the equipment. Do not apply complex, hypothetical theory that you do not understand.
- Check system inputs. Don't make assumptions. There may be a situation when inadequate levels or values are available.
- Similarly check system outputs or outputs at various stages.
- In such situations, split the system into smaller sub-units and only check suspected blocks or circuits. This helps in pin-pointing a defect.
- When a fault has been identified, more than half of the work is done. Ascertain why it could have occurred and record the findings, corrective and preventive measures taken (preferably in the equipment's respective history sheet); this will help in the future.

Various types of instruments are available for testing electrical circuits. The ones you choose will depend on the type of circuit and its components.

A common test instrument which is invaluable to a troubleshooter is a multimeter. It is capable of measuring voltage and resistance with some meters capable of other measurements such as current, capacitance and frequency.

A meter that is capable of measuring current, voltage and resistance is also called an AVO meter (ampere volt ohm meter) You must be able to determine what type of test instrument to use, when and where to use it and how to safely take readings with it.

The following procedure describes the method used to ensure that measuring equipment for critical and essential equipment is maintained, tested and calibrated within the manufacturer's instructions and guidelines. The Chief Engineer / Superintendent are responsible for the calibration of measuring equipment.

3.1 Procedures

- Pressure gauges, thermometers, voltmeters are for normal assessment purposes. They are replaced or repaired if they become defective.
- Measuring instruments used by personnel are for checking purposes only. Instruments considered critical and essential for calibration are to be checked before use to confirm accuracy and to be verified by calibration annually.
- Where there is a contract requirement, the measuring instrument used is to be regularly calibrated at the contract specified intervals.
- The Measuring instruments are to be calibrated by a specialist firm. The reference instrument used in the calibration shall itself be certified to be calibrated to nationally recognised standards or the basis used for calibration shall be documented.
- A record of measuring equipment with dates when equipment was calibrated and certificates are to be retained by the Chief Engineer and recorded in the Maintenance reports.
- If measuring equipment is found to be defective or out of the permissible limits during calibration, all equipment which has been tested with this instrument to be re-tested for accuracy.
- Calibration Certificates are to be kept for 10 years.

4 Understanding How to Use Blue Prints and Diagrams

Some of the key features to be determined from these are:

- How should the circuit operate?
- What kind of features does the circuit have?
- What voltages should you expect at various points on the circuit?
- Where are the components physically located?
- How are the components wired together?

About the Author

43 years in the Maritime and Energy Industries; Author / Co-author of 80 Books; Chartered Engr, FIE, MIET (UK), MLE[SM] Harvard Square (USA); Joint Inventor with a Patent for Supervised BNWAS; Promising Indian of the Year in 2017;

Email: elstan.a.fernandez@gmail.com

HERITAGE HOURGLASS: A SAGA OF *NARI SHAKTI* IN INDIAN WATERS

Amruta Talawadekar, Maitre Shah

Introduction

Being peninsular in nature, India traces its maritime roots from prehistory. From occupation to communication, Indians have been dependent on the surrounding waters for their livelihood. Lying in the heart of the Indian Ocean, the Indian Peninsula soon became a home for several flourishing port cities which were ruled by the hereditary monarchs. Trade played a crucial role in the economy of the kingdom and often led to brawling among kingdoms and foreign invaders. Thus, protecting the kingdom and its trade interests was immensely important and a maritime force was imperative. Due to predetermined standards of society, the term, 'force' is generally associated with men and we often hear about the bravery of men. In spite of this, Indian history is evident of women who have showcased their strength, relentless perseverance and able leadership skills across multifaceted sectors. In the maritime domain too, women's contribution cannot be overlooked. The feats of the women in history, showcasing their maritime prowess is rather overshadowed or hidden deep inside the annals of history. Through this essay, let us salute the bravery of these distinguished women who etched their names in India's maritime history.

The Beginning of a Revolutionary

Women have proved to be avid warriors and brilliant administrators while securing a place in history, be it in the field of warfare, politics, art, literature or business among others. Women have been an influential part of the society contributing immensely to every field. Age and gender are social constructs that are defined by society. On the maritime frontiers too, the sea doesn't recognise gender and women have proved that the chauvinism in the field of seafaring should be kept at bay. A number of women have proved themselves in the field of shipping, warfare, aviation and sailing among other multidimensional genres. Though the history of the contribution of the ancient Indian women in the maritime field is yet to be discovered, literary sources do provide us with the names of some medieval queens who have contributed immensely to the maritime fraternity.

Abhaya Rani: The Fearless

Written records of women maritime prowess can be seen as early as the seventeenth century with the accession of Rani Abbakka to the throne of Ullal, Tulu Nadu (present day Karnataka). By providing strong resistance to the European powers, she became India's first woman freedom fighter. The 'Age of Discovery' opened new sea routes and the Portuguese became the first Europeans to establish their foothold in India in 1498. Ullal, the capital of the Chowta dynasty, nestled between the Western Ghats and the Arabian Sea. Due to its strategic location, the thriving port town of Ullal came under the target of the Portuguese. Princess Abbakka, the niece of King Thirumala Raya, was the heir to the throne.

The king educated Princess Abbakka in sword fighting, archery, cavalry, military strategy, diplomacy and all other subjects of statecraft from a very young

Thus, protecting the kingdom and its trade interests was immensely important and a maritime force was imperative. Due to predetermined standards of society, the term, 'force' is generally associated with men and we often hear about the bravery of men

age. When Abbakka was crowned, the Portuguese levied high taxes on the kingdom of Ullal. Exasperated at the unfair demands, Rani Abbakka refused to cooperate with them.

The non-compliance to the Portuguese demands led to a major conflict. She built her own maritime force with *Mogaveeras* (a Muslim fishermen community) and *Billava* archers and *Mappilah* oarsmen. The first battle took place in 1556, which ended in an uneasy truce. Two years later, in 1558, another battle took place between the Portuguese and Rani Abbakka. During this battle with the support of a strong army and her battle tactics, Ullal Queen was able to push the Portuguese back once again. During the next battle, the Portuguese army attacked Ullal and managed to capture the royal palace. However, the Queen of Ullal had already escaped. Along with two hundred loyal soldiers, she attacked the Portuguese in the dead of night and killed the general along with many of his soldiers.

Though the history of the contribution of the ancient Indian women in the maritime field is yet to be discovered, literary sources do provide us with the names of some medieval queens who have contributed immensely to the maritime fraternity

Image 1 Rani Abbakka
Source - Rani Abbakka Tulu Museum

Frightened by the ferocity of the attack, the remaining Portuguese troops retreated. In 1581, three thousand Portuguese troops supported by an armada of battleships attacked Ullal in a surprise pre-dawn attack. Rani Abbakka's piercing battle cry – "Save the motherland, fight them on land and the sea, fight them on the streets and the beaches, push them back to the waters" motivated her fleet till the end. Even though she was captured by the enemy, her bravery and patriotism earned her the title '*Abhaya Rani* or 'The Fearless Queen.' This legacy of bravery and patriotism towards the motherland was passed by Rani Abbakka to her daughters, who continued to protect the Ullal Kingdom. These daughters were also called Abbakka.

The Diplomatic Sovereign

The Malabar Coast was renowned in the European markets for the availability of premium quality spices especially pepper. The Kingdom of Attingal (present day Kerala) was known to produce the finest pepper and the queen who ruled Attingal was known as the 'Queen of Pepper'. The Queen of Attingal during this period was Aswati Tirunal Umayamma.

In 1662, the Dutch had signed a treaty with Raja Rama Varma, Raja of Travancore, by which they acquired the monopoly of pepper and cinnamon trade. Assuming that the English would help them restrain the Dutch and earn more profits, Rani Umayamma invited the English to open a factory in 1678. The friendly trade association between Attingal and the English was not accepted by the Dutch who started attacking the English ships and disturbed their trade. Being a port town, both the Dutch and English were keen to establish their foothold there. Rani Umayamma tactfully managed to maintain her dominance over the region's maritime trade through negotiation and treaties till Raja Marthanda Varma made the Rani of Attingal sign the Silver Plate Treaty of 1731.

Image 2. Sumati Morarjee.
Source:https://prabook.com/web/sumati.morarjee/1875789

A Maritime Entrepreneur

Women not only set their benchmark in defence but also in the field of shipping and entrepreneurship. Shipping has been a crucial part of the maritime industry and has been rigorously affected by the economic and political changes in the country which requires knowledge about different fields. Sumati Morarjee was the daughter-

in-law of Narottam Morarjee, an Indian businessman and founder of Scindia Steam Navigation Company Ltd. After his sudden demise, she and her husband took over the company and she went on to become its Executive Director. With her keen intellect and vast knowledge, Sumati often offered insights to her father-in-law on business affairs. So, she was well aware of how things worked at sea, the mechanism of ships and the difficulties faced at high seas. During her tenure as the Executive Director, the annual profits historically rose and 1949-1969 came to be known as the 'Sumati era'. Her vision helped in the upliftment of the shipping industry as well as the people. She was a woman of avid qualities of leadership, entrepreneurship and competence.

Women's Royal Indian Navy (WRIN)

Image 3. Chief Officer Margaret L Cooper with Second Officer Kalyani Sen at Rosyth, UK.
Source: https://wrens.org.uk/womens-royal-indian-naval-service-established-during-ww2/

Image 4. Women's Royal Indian Naval Service (WRINS) at GHQ Delhi - 1945.
Source: https://defenceforumindia.com/threads/extremely-rare-picture-of-an-indian-lady-in-royal-navy-uniform.29065/

India by the twentieth century came under British rule and was part of the Queen's provinces. Manning of the maritime borders was under the Royal Indian Navy (RIN). During World War II, with a rising requirement of naval personnel the RIN began inducting civilians on a large scale to fill up onshore and offshore jobs including both men and women. The Women's Royal Indian Naval Service (WRINS) that was set up in February 1944 as a part of the Women's Auxiliary Corps (India) became a pioneering step towards empowering women in the field of defence. They played a crucial role in strategising, documenting and decoding secret messages for the war. They were given duties like cipher work, decoding secret messages, manning switchboards and were trained in gunnery tactics, maintenance of equipment etc. By 1952, nearly two third women in the WRIN were of Indian Nationality. The sari and shirt attire of the WRINs symbolised the 'new Indian woman' linking 'modern ideology while maintaining the desire to preserve Indian culture'. This proved to be a revolutionary in the armed forces. As part of the training protocol, Second Officer Kalyani Sen travelled to the United Kingdom for a two months study visit with her English counterparts thus becoming the first Indian service woman to do so.

Contemporary Women Feats

Post-independence, till 1992, WRIN became the only armed force in India to have a women's wing. Eventually it began inducting women for selected branches of the Indian Navy (IN). Over the years the branches expanded and today we have women in the fields of Air Traffic Control, Observers, Law, Logistics, Education, Naval Architecture and the Naval Armament Inspectorate. Dr Barbara Ghosh became one of the first Indian women to have attained the rank of a commander. She was also the first woman medical officer to have received a permanent service commission. Subsequently, Surgeon Vice Admiral Punita Arora PVSM, SM, VSM became the first woman to reach the second highest rank as the Lieutenant General and the first female Vice Admiral in 1968.

Capt. Radhika Menon became the first Indian Female Captain of an Indian Merchant Navy Ship in 2012. In 2015, she led a dangerous rescue mission in the Bay of Bengal when a boat was capsised due to engine failure and breakdown of the boat's anchor as a result of a sea storm. She was honoured with the International Maritime Organization (IMO) Award for Exceptional Bravery at Sea in 2016. The Indian Coast Guard in 2017 inducted women officers for combat and patrolling roles onboard KV Kuber, becoming the first Indian force to do so.

In 2018, six women officers led by Lt Cdr Vartika Joshi (Retd) circumnavigated the world in a sailboat becoming the first women crew in India to undertake such an adventurous task. They displayed relentless spirit and passion to undertake a 254-day long voyage in uncertain conditions in their sail boat *Tarini* or the saving goddess.[1] In 2019, Lieutenant Shubhangi Swaroop was inducted as the first woman pilot in the Indian Navy. Cdr Rajeshwari

Image 5. Tarini image: All women crew onboard INSV Tarini
Source:https://www.thehindu.com/news/national/navys-women-team-sets-sail-from-goa-to-circumnavigate-globe/article19655415.ece

Kori (Retd) featured in the Limca book of records for being the first Indian woman in the Asian Subcontinent to be sent on board an Indian Naval Warship INS *Jyoti* as a Logistics Officer in 1997. On 21 September 2020, Sub Lt. Riti Singh and Lt. Kumudini Tyagi became one of the first women to join as an 'Observer' (Airborne Tactician) in the Indian Navy's helicopter stream. Ms Reshma Nilofer is the world's first and only woman Marine Pilot currently working at the Shyama Prasad Mukherjee Port Trust, Kolkata.

Conclusion

As rightly said, the sea doesn't discriminate between genders. Women across centuries have proved their capabilities, dedication and relentless spirit in combat and non-combat roles. Indeed, these women form an integral part of the rich maritime heritage who have created an inspirational path for others to follow.

References

1. Sanchari Pal. The Forgotten Story of Rani Abbakka Chowta: The Fearless Warrior Queen of Tulu Nadu. *The Better India.* Accessed and retrieved through - *https://www.thebetterindia.com/115196/rani-abbaka-chowta-ullal-tulu-nadu-karnataka/*
2. Leena, P. K. (1985). Rani Of Attingal and The English in Travancore. *Proceedings of the Indian History Congress,* 46, 364–372. Accessed and retrieved through - http://www.jstor.org/stable/44141376
3. *Ed. N. G. Jog. (1970) Sumati Morarjee: Felicitation Volume. India: Smt. Sumati Morarjee Shashti-Abdi-Poorti Celebration Committee.*
4. Women's Royal Indian Naval Service established during WW2. https://wrens.org.uk/ Accessed and retrieved through *https://wrens.org.uk/womens-royal-indian-naval-service-established-during-ww2/*
5. *https://www.indiannavy.nic.in/content/navika-sagar-parikrama-circumnavigating-globe-indian-built-sail-boat-insv-tarini-women-naval*

About the Authors

Amruta Talawadekar is an Architect by profession with a M.Arch in Architecture and Urban Conservation. As a Senior Research Associate at the Maritime History Society, Mumbai, she looks into the research and conservation of built heritage lying within the maritime domain. Living in Mumbai, her keen interest lies in the maritime history of Mumbai. Being a heritage enthusiast and a technical professional, she is inclined towards the ship building practices and techniques of India. She has presented papers at various national and international platforms and has been a regular contributor to the MER Journal.

Email: amruta.rab@mhsindia.org

Maitre Shah is a student at St. Xavier's College, Mumbai, pursuing her post-graduation in Ancient Indian Culture and Archeology. Her keen interest lies in Epigraphy, Numismatics and Manuscriptology and wishes to pursue further research in the same field. Being an avid reader, the multi facet Indian culture and its rich history inspires her to discover the hidden aspects in the annals of history. She is currently working as an Intern at the Maritime History Society, Mumbai.

GOING ASTERN INTO MER ARCHIVES

MER... Four decades back...
The March 1983 Issue

The March 1983 sports a cover with the launch of a sea cadet training ship. Toi whom was this for... IN or the MN and what happened to this vessel? Someone may whet my curiosity. We pause at the Editorial announcing the shift to new office premises at Maker Tower.

As we dig in tot eh issue, the first hot topic is the one on electrical fires. I am tempted to snip a whale's portion of the article but I will leave your interest lingering with the Figures. Apparently, it is an edited version of the Transaction of IMarE (TM); Vol. 95, 1983, Paper 38.

The next one is on the ever-fascinating Stirling engine, which was modelled much before the Carnot engine. I leave it to you to work around the cold/hot sides displacement and the piston doing work. Then there is news on China's fleet expansion, sail assisted research ship, and a write-up on RO for producing water. An analytical article to spend time on is on the CP propellers.

The Postbag has some feedbacks. The discussions might appear to be on outdated technologies but a serious reading would bring out some knowledge relevant for today's operations: The control of secondary air for boiler combustion and the CPP pitch shedding issue aggravated by a hydraulic valve block are good takeaways (for want of discussion-connection, the full 'Postbag' has been extracted.

Shipboard fires: the electrical connection

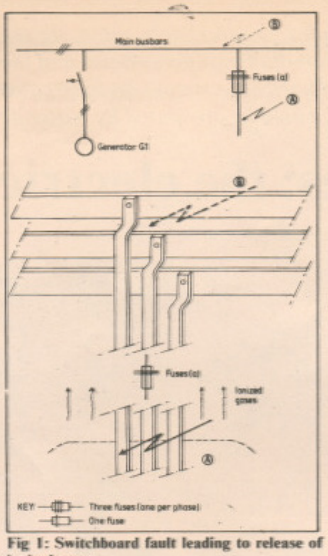

Fig 1: Switchboard fault leading to release of ionised gases.

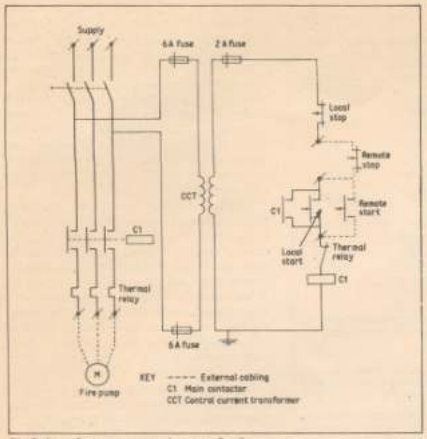

Fig 2: Unsafe remote control system for fire pump.

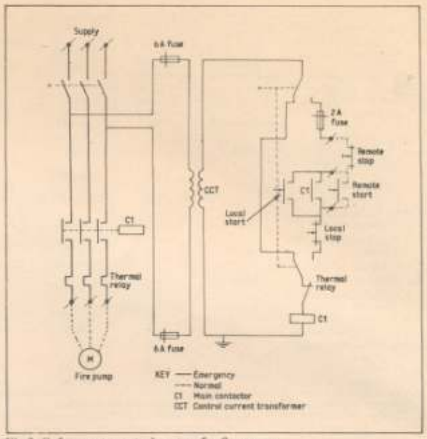

Fig 3: Safe remote control system for fire pump.

Fig 4: Standard bulkhead or deck gland box.

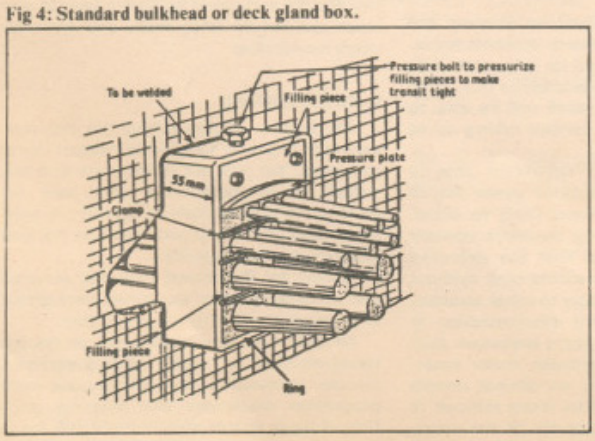

Fig 5: Bulkhead penetration for 'A' class penetration.

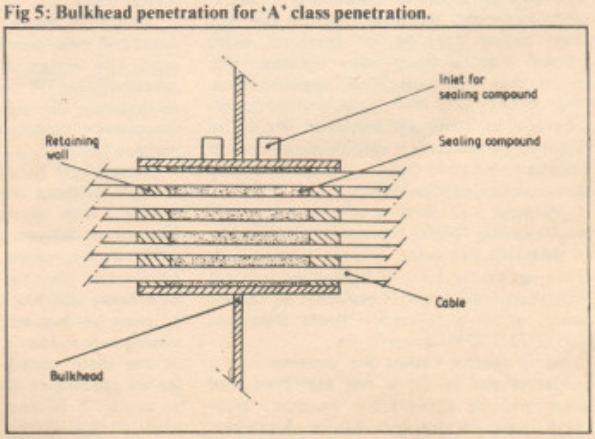

Stirling stuff, but not for students

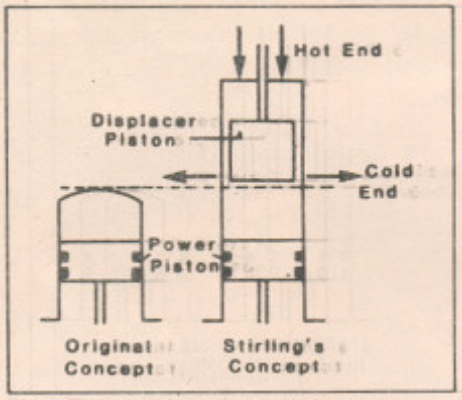

Fig 1: The role of the displacer piston.

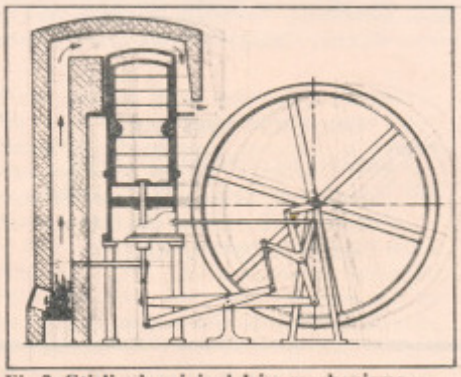

Fig 2: Stirling's original drive mechanisms.

Fig 3: Rhombic drive.

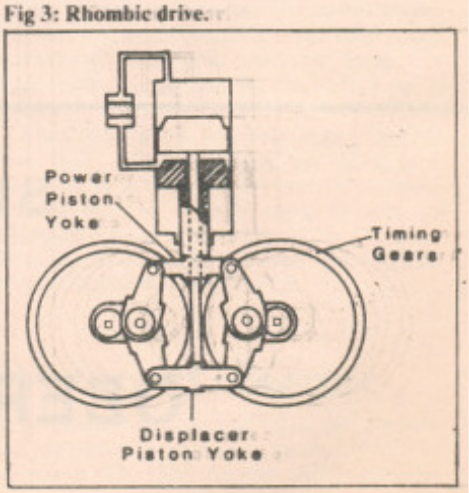

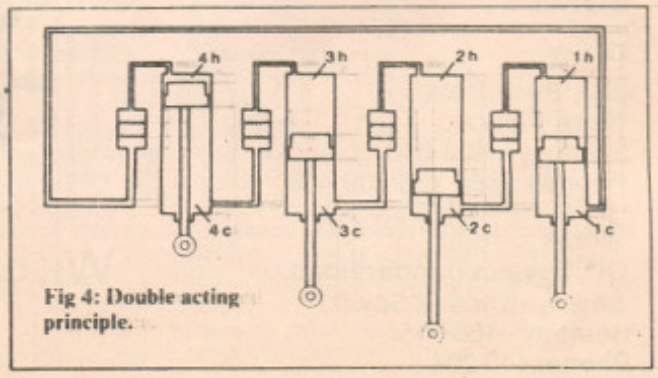

Fig 4: Double acting principle.

POSTBAG

Coal-fired ships

Sir,
I read with interest Mr H O Walker's proposals regarding the control of coal-fired ships (MER October 1982).

Whilst the system put forward by Mr Walker is very similar to that proposed by me and published in your September 1980 edition, I am, however, at a loss to understand why he has chosen to omit control of overfire or secondary air.

On falling load, uncontrolled secondary air becomes a progressively greater proportion of the total air requirement. The end result is reduced air flow through the grate, a caking fuel bed, and a thoroughly dirty fire.

Coal-fired boilers can be dirty as load is reduced, hence the need for some form of opacity control or monitoring. This helps in two ways. (1) It overrides the oxygen trim via an auctioneer to clean up the stack. (2) It increases the gas velocity through the boilers and assists the cyclone grit separators to work more efficiently.

Its disadvantage is to provide more air than is actually required and thus, increase heat loss to the stack. However, this is only short-term.

Despite general opinion, spreader stoker boilers are not all that slow to respond and I cannot help but think that the complexity of dump valves and suitably constructed condensers are an over complication. My experience in power stations is that the dumping of high-pressure steam into a condenser is not without its problems.

It would appear that a cp propeller installation, plus some co-operation in transferring coal during manoeuvring, would assist in keeping load up. I understand the former consumes about 12 per cent power in the neutral thrust position.

Whilst sliding-pressure operation has its advantages in minimising throttling losses I feel that, if the turbine valving is properly sized, the sliding pressure is an unnecessary complication.

The Broken Hill Co in Australia operated two automatically controlled coal-fired vessels for many years and, to the best of my knowledge, their simply controlled spreaders worked very well.

Recent published papers indicate that we are tending to over complicate what is basically a simple and safe process. Please, let us not re-invent the wheel of coal firing.

G Edwards

Sydney, Australia

Mr Walker replies

The omission of the overfire air control loop from my scheme was an oversight on my part and I would endorse Mr Edwards' comments that control of the secondary air is required to produce turbulence and complete combustion.

I find the objections to the application of 'sliding pressure control' and the use of dump condensers quite surprising. The additional elements in the loop control system required by the sliding pressure loop are minimal and should not cause any problems.

The advantages of the sliding pressure system have been demonstrated on oil-fired steam ships and have given improved fuel economy. It is difficult to imagine how the sizing of the turbine valves can influence the system efficiency. The improved performance of the boiler at reduced loadings should more than compensate for any throttling losses in the manoeuvring valves.

H O Walker

Blaby, Leicester

Feedback

Sir,
Your comment in the December issue, following Mr Schreiber's suggestion regarding 'feedback' on the problems and weaknesses of equipment, is most encouraging.

Seemingly the marine industry is well endowed with enlightened suppliers who make it their business to 'keep their feet on the engine room floor plates' and keep in close touch with the engineers who walk them. This has ever been a cardinal rule of any really successful marine equipment supplier.

H C R Trewman

Westinghouse Electric Corp,
Sunnyvale, USA

. . . fed back

Sir,
The following problem was experienced with an electro/pneumatic/hydraulic main engine and cp propeller control system on a new ship.

The propeller would not shed pitch automatically as the engines approached overload. Investigations were made to establish the cause but unfortunately there were several factors which obstructed the finding of an early solution.

The line diagrams in the manufacturers' manual were too small to be studied without incurring blurred vision and they gave no details of the component parts. The line diagrams in the shipbuilder's control and instrumentation specification defied logic. Furthermore, the New Zealand agents were unaware that their principals had produced this control system.

Because main engine power was used when discharging cargo, the opportunity to work on the system was limited. It was not until some eight months after delivery of the vessel that an opportunity arose to tackle this fault.

Starting at the pitch controller, line diagrams were made, components withdrawn, dismantled, sketched and reassembled (the shipyard diagrams were found to be in error).

Three working days gave sufficient understanding of the system to realise that the pressure regulators had been wrongly set; this was quickly rectified.

These efforts helped the situation, but only when the starboard main engine was on propulsion duty by itself. The last barrier was found to be a hydraulic valve block mounted in reverse on the line from the port main engine governor to the pitch-shedding mechanism. A few minor adjustments to restrictor valves had the system working.

Less than a week later a copy of a letter from the shipbuilders arrived on the Chief Engineer's desk stating that the pitch shedding mechanism had worked well on trials!

Makers' manuals are, all too often, substandard and do not give sufficient information to operate equipment correctly, trouble-shoot or rectify problems. On the vessel referred to, I found it essential to have a 'how it works' file on various items of plant; using the 'sketch and describe' format.

I do not believe that sea-going engineers have few problems or that they are unwilling to share solutions through MER. I do believe that they may be reluctant to submit, to a learned society, problems that have had, like mine, mundane solutions which need not be supported by pages of graphs and calculations.

T Carson

Wellington, New Zealand

● *This journal is aimed at many practical people: no solution is too mundane if it concerns a real problem* —Editor

EVENTS

17–18 March: Semi-submersibles—the new generations. (International symposium). London Tara Hotel. RINA. Tel: (01) 235 4622.

21–25 March: Expoship London 83. Barbican, London. Seatrade Conferences. Tel: (0206) 45121.

29–31 March: Annual National Maritime Show. (Conf & Exhib). Baltimore, Maryland. NMS, 10703-A Stancliff, Houston, TX 77099. Tel: (713) 8798929. Tlx: 790821.

12–15 April: Coatings and surface treatments for corrosion and wear resistance. (Conf). Newcastle upon Tyne Polytechnic. Tel: (0632) 326002 ext 330.

13–15 April: ChemSea 83. (Conf and Exhib). London. Conference Secretariat. Tel: (01) 283 2922. Tlx: 884008.

19–22 April: World Dredging Congress. (Conf). Singapore. Conference Organiser, World Dredging Congress, BHRA Fluid Engineering. Tel: (0234) 750422. Tlx: 82505.

20–21 April: Wartime adaptation of merchant ships. (Symposium). London. British Naval Equipment Ass'n. Tel: (01) 247 7566.

1–4 May: High-speed Surface Craft 83. (Conf). London. Conference Organiser, 51 Welbeck Street, London.

We invite observations, discussion threads from readers, taking cues from these sepia-soaked MER pages – Hon.Ed.

IME (I) GOVERNING COUNCIL, BRANCH AND CHAPTER COMMITTEE ELECTIONS 2023-25

With elections for The Institute of Marine Engineers (India) approaching, we would wish to notify all Corporate Members of the following procedures:

SCHEDULE

- Notice of the entire process of election shall be intimated through electronic media ONLY
- Soft copy of the Nomination forms will be sent through mass e-Mail and can also be downloaded from the IME(I) website and returned to the Election Officer.
- Soft copy of the Nomination papers for Council elections will be mailed by 15th May 2023 to the Members email id which is registered in the records of the IME(I).
- Nomination papers for the Council are to be received in the Institute's office by 15th June 2023 to the email id: ***electionofficer@imare.in***
- Last date for withdrawing nomination is 30th June 2023.
- The scrutiny of nomination papers for the Council to be completed by the Election Committee by the 5th July 2023.
- Election Officer after scrutiny will publish the CVs of the eligible candidates on IME(I) website.
- The election window for eVoting will remain open from 15th July to 1st September 2023.

E-VOTING

As a corporate member you can exercise your franchise at the forthcoming elections at IME(I), using the standard Ballot **through e-Voting ONLY**.

Two options would be available for both the elections i.e. for Head Office (HO) as well as the Branch Level (if the election takes place for the Branch level). Overseas Members will get Option only for elections at HO level.

Members will get the e-Voting Link **ONLY on** their e-Mail registered in the records of IME(I) as on 15th May 2023. Members may update their e-Mail ID / contact details by writing to the HGS at ***membership@imare.in*** latest by 15th May 2023.

USE OF WORKPLACE / OFFICIAL MAIL IDS

- Given that we have, in the past, had mass emails blocked at certain receiving (Organization) mail domain(s), treated as spam and, in some cases the blacklisting of the IME(I) domain, we would strongly recommend the use of personal email ids ONLY.
- The use of your personal mail would ensure that you do not miss any important communication relative to the election process.

Election officer
electionofficer@imare.in

MASSA Maritime Academy, Chennai

The Institute of Marine Engineers (India)

Electronic Engine Familiarisation Course (ME-Type Engine) Delivered online with Cloud access to ME Engine Simulator

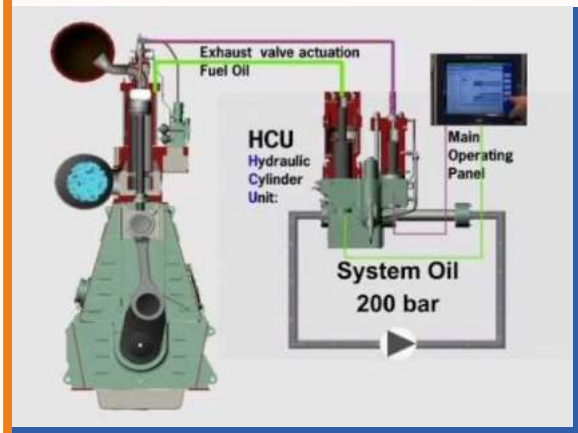

This 3 days course is designed for all Ship's Engineer Officers and Electro Technical Officers responsible for the operation of ME Engine. This course consists of technical lessons and practical instructions on the design, principles, operating procedures and maintenance activities for the safe, efficient and optimal performance of the engine system.

Course Aims and Objectives:

The course aims to provide practical understanding of the principles, design, operation and maintenance of the ME Engine System, enabling participants to safely and efficiently operate the engine and perform fault-finding in the control system.

Coverage / Program Focus:

This course deals with the following training areas:

- **Introduction to ME Engine**
- **Hydraulic Power Supply (HPS)**
- **Hydraulic Cylinder Unit (HCU)**
- **Engine Control System (ECS)**
- **Main Operating Panel (MOP)**
- **Standard Operation**

Entry Requirement / Target Group:

Entry is open to all Ship's Engineers and Electro Technical Officers with basic knowledge of diesel engines.

DATE & TIMING : **21st, 22nd, 23rd March 2023/ 18th,19th, 20th April 2023/ 23rd, 24th, 25th May 2023/ 20th, 21st, 22nd June 2023 8:00 am - 4:00 pm IST**

VENUE : Web Platform / Zoom**. APPLICATION LINK:** https://forms.gle/e4As7kCucR5xoJBm9

REGISTRATION & PAYMENT : Rs. 15,000/- /- per participant – inclusive of taxes.
For IME(I) Members 13,500/- per participant - inclusive of taxes.
Payment to be made to: https://imare.in/buy-online.aspx
(Under Category - Value added Courses) *10% discount available for IME(I) members*

FOR MORE INFORMATION : **@IME(I) - email:** training@imare.in, Ms. Anukampa
(M). 9819325273, **(T)** 022 27701664 / 27711663 / 2771 1664.
@ MASSA Maritime Academy Chennai - email: mmachennai@massa.in.net
Ms. Saraswathi, **(T)** 8807025336 / 7200055336 .

After registration and payment, please email the details of the receipt to: ***training@imare.in***

Published on 5th of every month
and Posted on 5th & 6th of every month at
Mumbai Patrika Channel Sorting Office, G.P.O., Mumbai - 400 001.
'Licence to post without prepayment'

"Reg. No. MCS/090/2018-20"
RNI No. MAHENG/2006/19917
W.P.P. Licence No.:
MR/Tech/WPP-336/ South/2018-20

IME(I) House, Nerul, Navi Mumbai